

# Improvement of the higher-order tensor renormalization group method

Satoshi Morita (ISSP, Univ. Tokyo)



東京大学 物性研究所  
THE INSTITUTE FOR SOLID STATE PHYSICS  
THE UNIVERSITY OF TOKYO



**CBSM<sup>2</sup>**

Challenge of Basic Science  
– Exploring Extremes through  
Multi-Physics and  
Multi-Scale Simulations



# Outline

- Introduction
  - Real-space renormalization based on TN
  - How to calculate a projector in HOTRG
- Calculation of higher-order moments by HOTRG
  - Renormalization of multi-impurity tensors
  - Finite-scaling analysis on q-state Potts model
- Entanglement filtering in HOTRG
  - HOTRG + Full Environment Truncation (FET)\*
  - Benchmark on 2d Ising model\*
- Summary

\* Unpublished results are removed in this PDF.

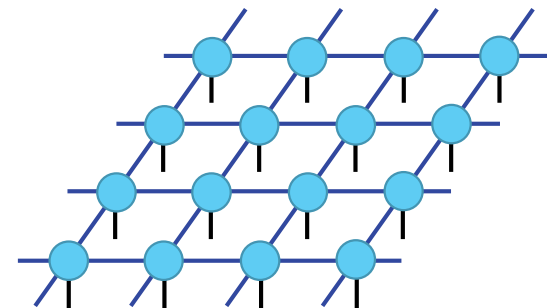
# Tensor network methods

## ○ Hamiltonian mechanics

- Wave function of many-body systems

$$|\psi\rangle = \sum_{i_1 \cdots i_N} C_{i_1 \cdots i_N} |i_1 i_2 \cdots i_N\rangle$$

$O(d^N)$  coefficients



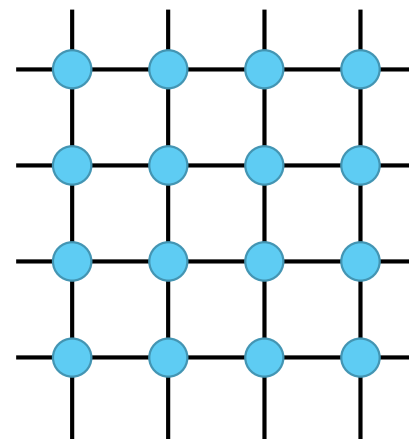
Approx. by tensor decomp.

## ○ Lagrangian mechanics

- Partition function (Action)

$$Z = \sum_{\{S_i\}} e^{-\beta H(\{S_i\})}$$

$O(d^N)$  terms



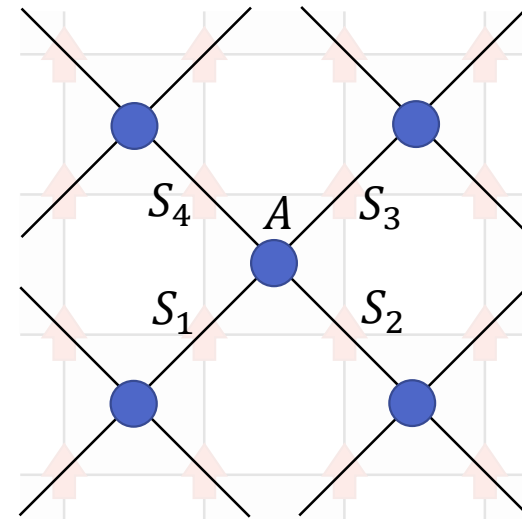
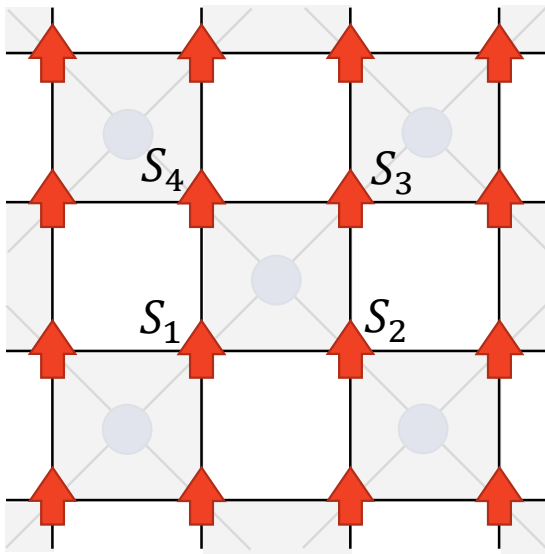
Representation by  
tensor decomp.

Tensor network representations reduce exponential computational cost to polynomial order.

# TN representation of the partition function

$$Z = \sum_{\{\sigma_i\}} \prod_{ij} e^{K\sigma_i\sigma_j} = \text{tTr} \left( \bigotimes_{x=1}^N A \right)$$

Sum over states    Tensor contraction



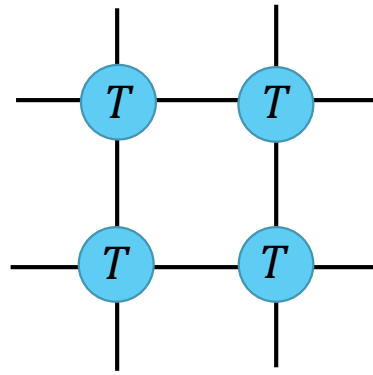
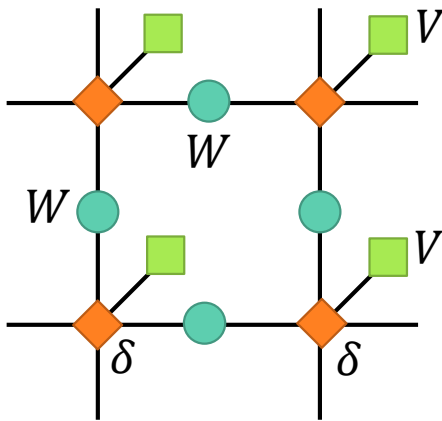
Ising model     $A_{S_1 S_2 S_3 S_4} = e^{K(S_1 S_2 + S_2 S_3 + S_3 S_4 + S_4 S_1)}$

- Tensor index corresponds to spin direction.
- One tensor contains two spin.
- In higher dimensional systems, a tensor has many indices ( $=2^d$ ).

# TN representation of the partition function

$$Z = \sum_{\{\sigma_i\}} \prod_{\langle ij \rangle} W_{\sigma_i \sigma_j} \prod_{i=1}^N V_{\sigma_i} = \text{tTr} \prod_{i=1}^N T_{x_i y_i x'_i y'_i}$$

Sum over states      Tensor cont.



$$T_{xyx'y'} = \sum_{\sigma} X_{\sigma x} X_{\sigma y} X_{\sigma x'}^* X_{\sigma y'}^* V_{\sigma}$$

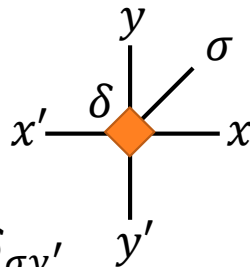
Local Boltzmann factors

$$W_{\sigma\sigma'} = e^{-\beta h_{\sigma\sigma'}}$$

$$V_{\sigma} = e^{-\beta h_{\sigma}}$$

Kronecker's delta

$$\delta_{xyx'y'} = \delta_{\sigma x} \delta_{\sigma y} \delta_{\sigma x'} \delta_{\sigma y'}$$



$$W \stackrel{\text{ED}}{=} U \Lambda U^{\dagger}$$

$$X = U \sqrt{\Lambda}$$

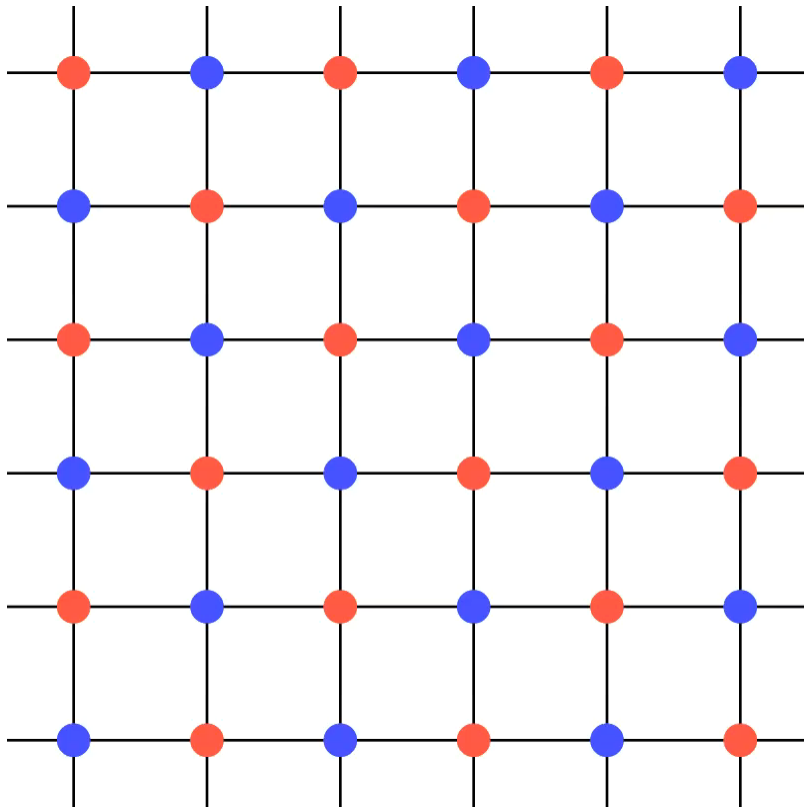
- Bond index is index of eigenvalue.
- Spin is already traced out.
- One tensor contains one spin.
- # of indices is  $2d$ .

# Real-space renormalization group

## ○ TRG

Tensor Renormalization Group

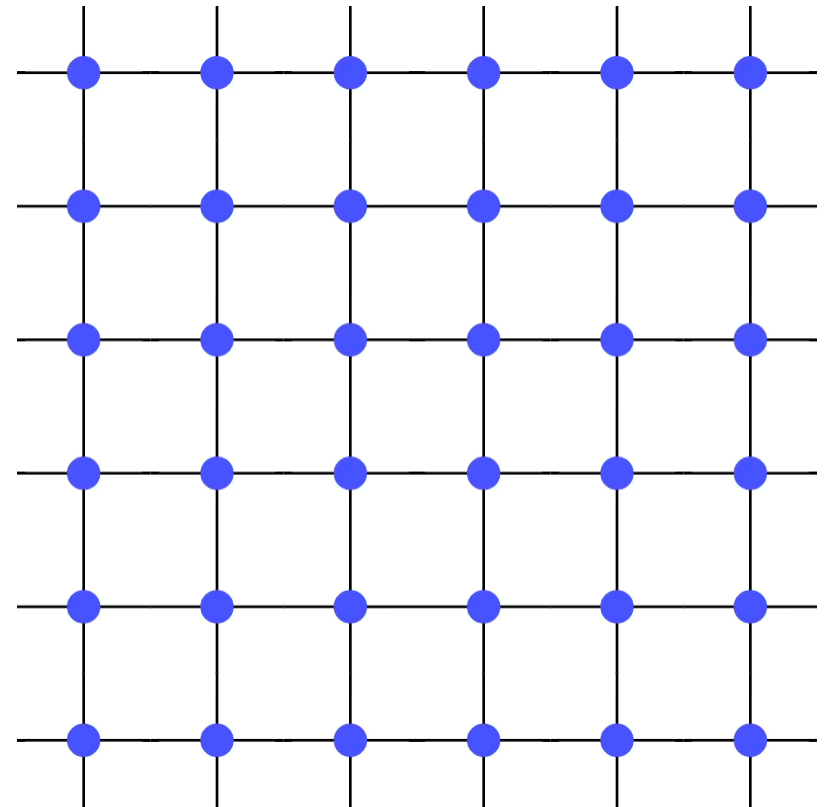
Levin, Nave (2007)



## ○ HOTRG

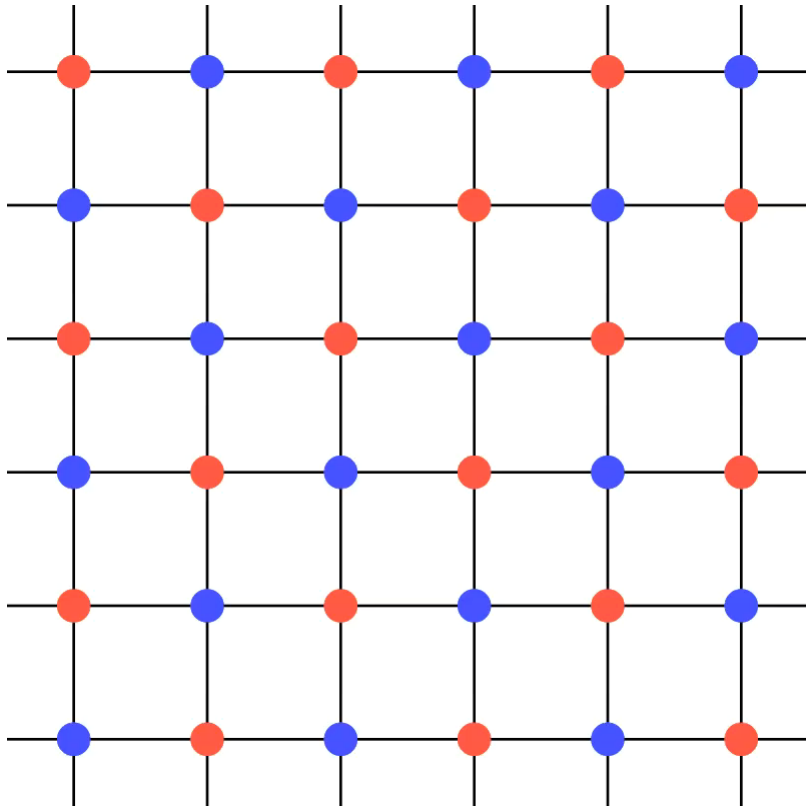
Higher-order Tensor Renormalization Group

Xie, et al. (2012)

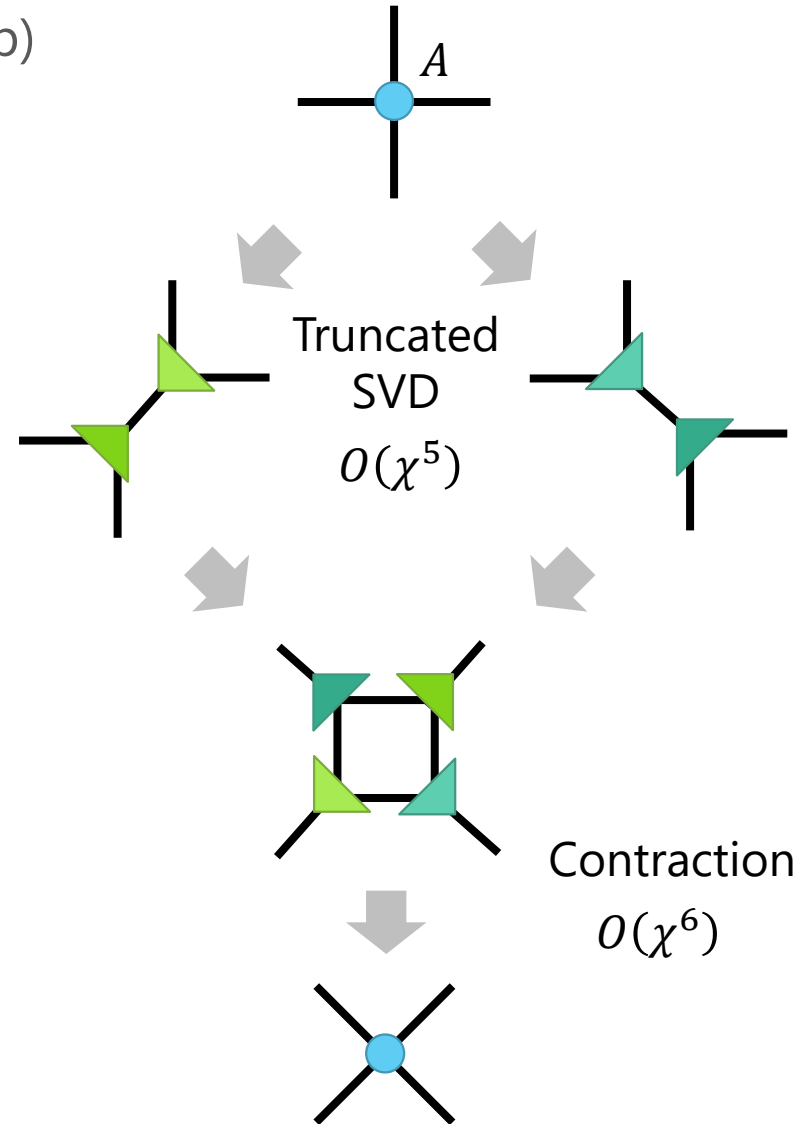


# Real-space renormalization

- TRG (Tensor Renormalization Group)  
Levin, Nave (2007)

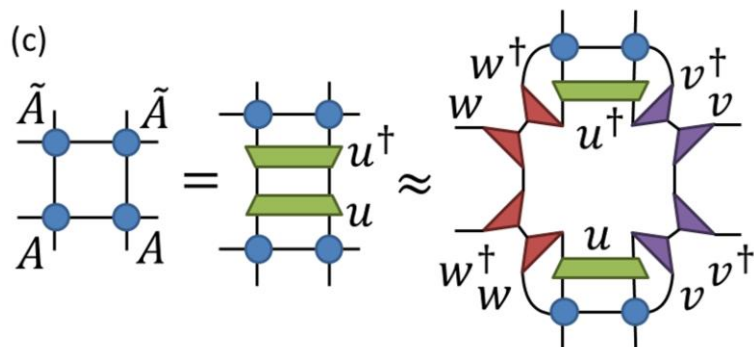


Decomposition & Contraction

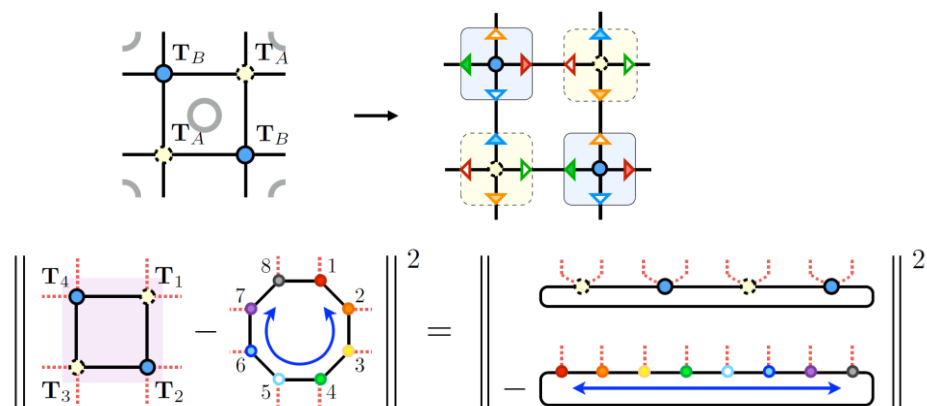


# TRG-base methods

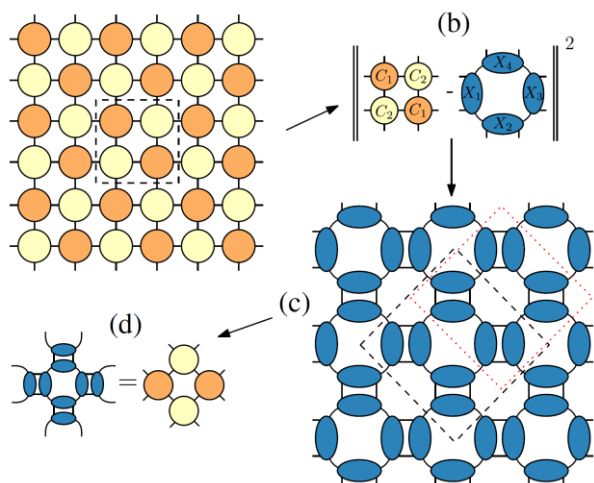
- TNR (Tensor Network Renormalization) Evenbly, Vidal (2015)



- Loop-TNR Yang, Gu, Wen (2017)



- TNR+ Bal, et al. (2017)



- $O(\chi^5)$  algorithms

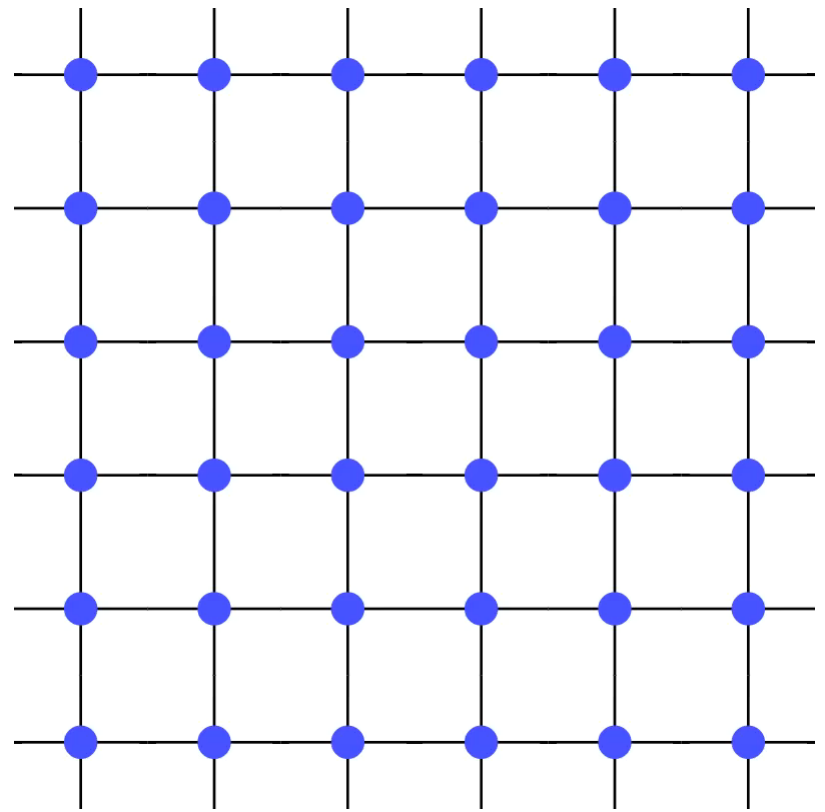
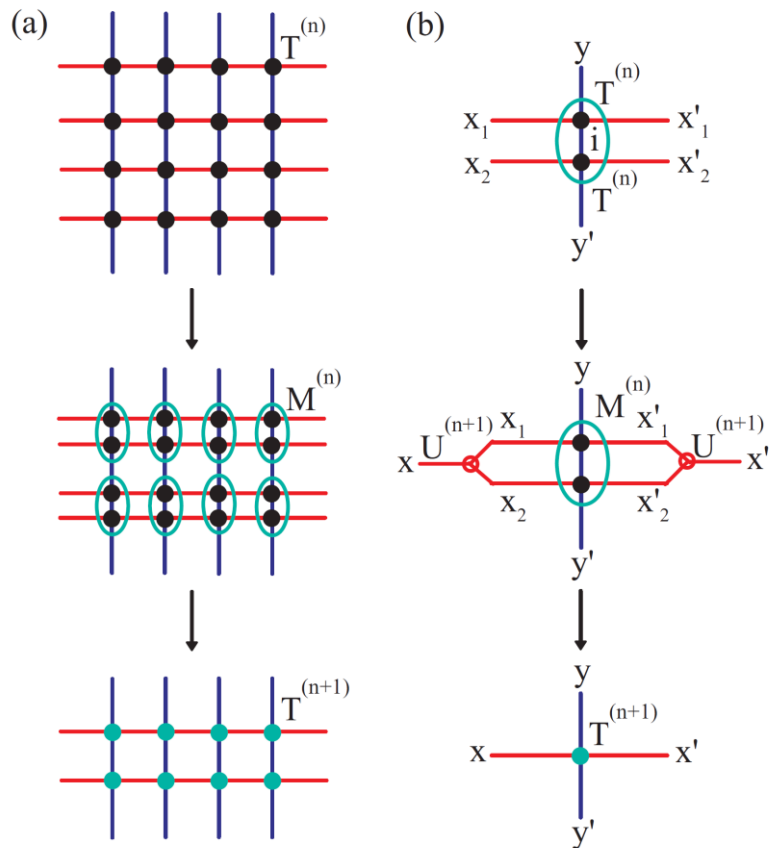
- TRG + Randomized SVD  
SM, Igarashi, Zhao, Kawashima (2018)
- Projectively Truncated TRG  
Nakamura, Oba, Takeda (2019)

Only for 2-d systems



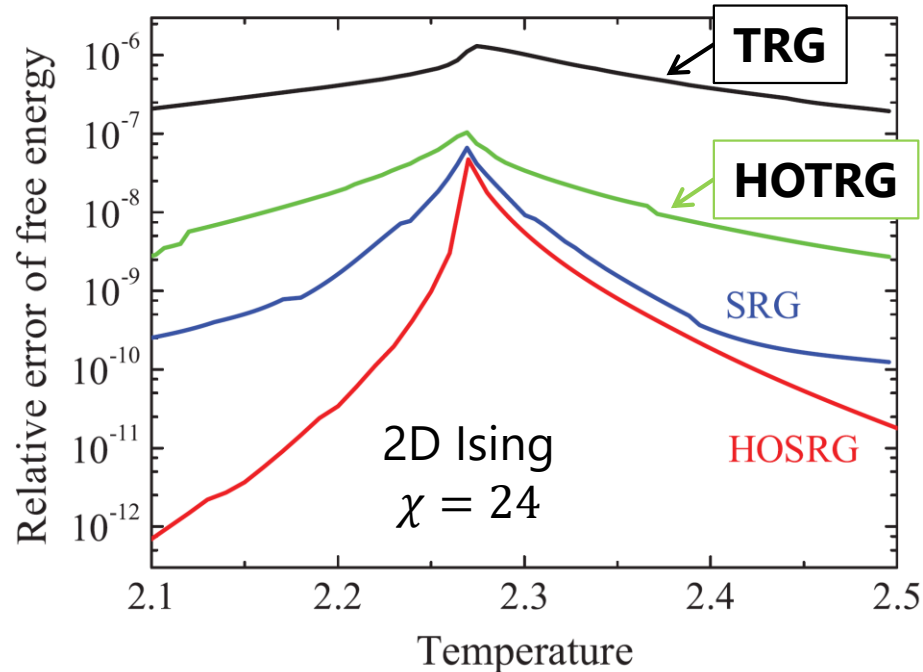
## ○ Higher-order Tensor Renormalization Group

Xie, et al. (2012)



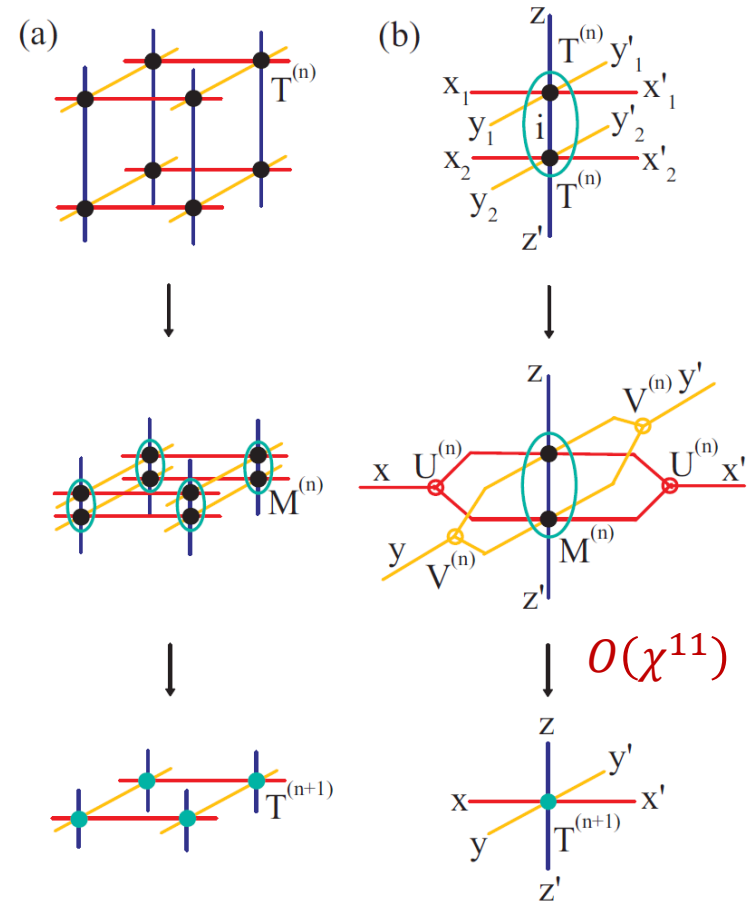
# Advantage of HOTRG

## ➤ Accuracy



- Conservation of lattice structure
- No tensor decomposition

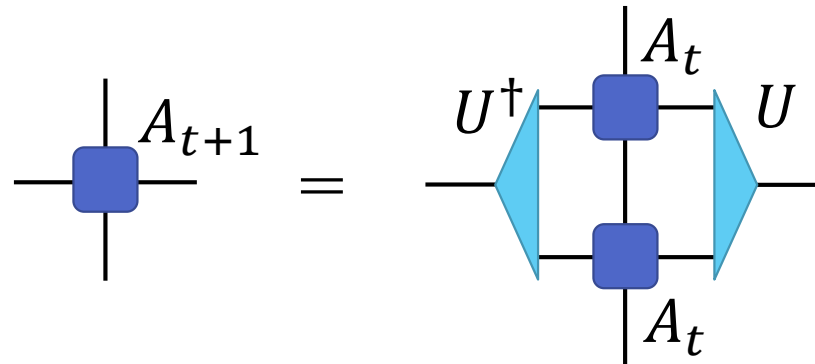
## ➤ Higher-dimensional systems



- ✓ 3-state Potts model on cubic lattice  
Wang, et al., (2014) [arXiv:1405.1179]

# Key parts of HOTRG

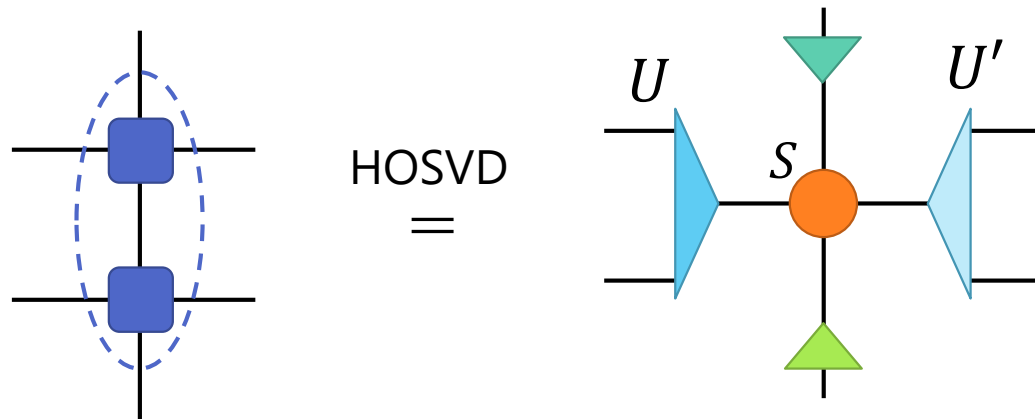
## ○ Renormalization



CPU cost:  $O(\chi^7)$   
Memory:  $O(\chi^4)$

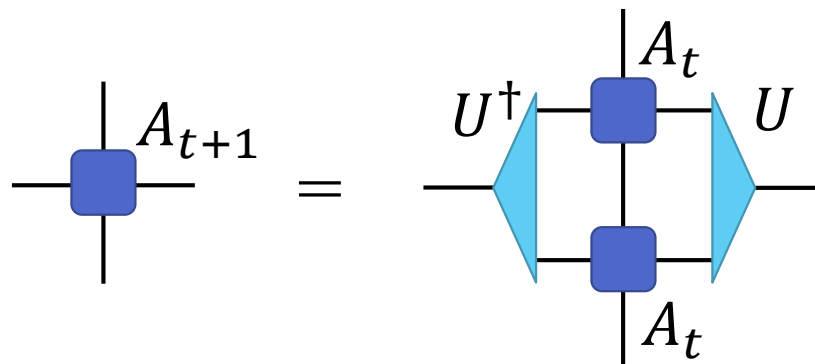
## ○ HOSVD (Higher-Order Singular Value Decomposition)

➤ truncated Tucker decomposition



# Key parts of HOTRG

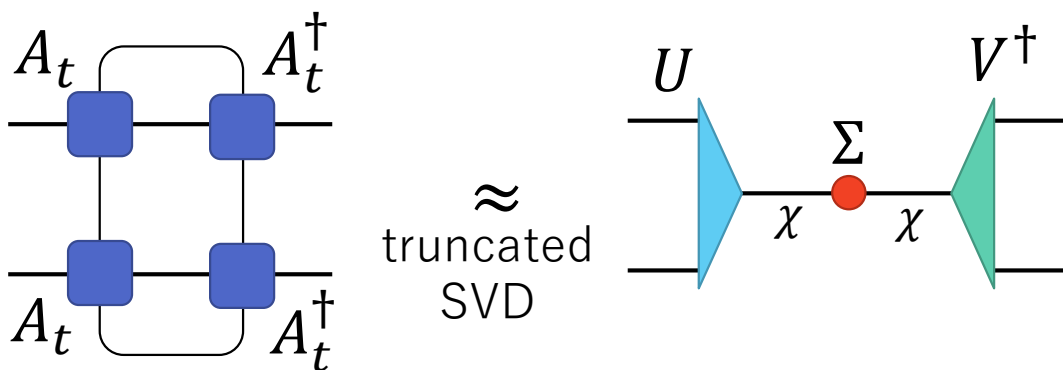
## ○ Renormalization



CPU cost:  $O(\chi^7)$   
Memory:  $O(\chi^4)$

## ○ HOSVD (Higher-Order Singular Value Decomposition)

➤ truncated Tucker decomposition



CPU cost:  $O(\chi^6)$

# Optimal Projector for 2x2 Cluster

## ○ Problem

$$\Delta = \min_{P, Q} \left| \begin{array}{cc} T_1 & T_3 \\ T_2 & T_4 \end{array} \right| - \left| \begin{array}{cc} P_L & P_R \end{array} \right|^2$$

The diagram shows a 2x2 grid of blue circular tensors labeled  $T_1$  (top-left),  $T_2$  (bottom-left),  $T_3$  (top-right), and  $T_4$  (bottom-right). To the right, a minus sign is followed by a vertical bar containing two orange trapezoidal tensors labeled  $P_L$  and  $P_R$ , with a superscript 2 outside the bar.

Lower bound

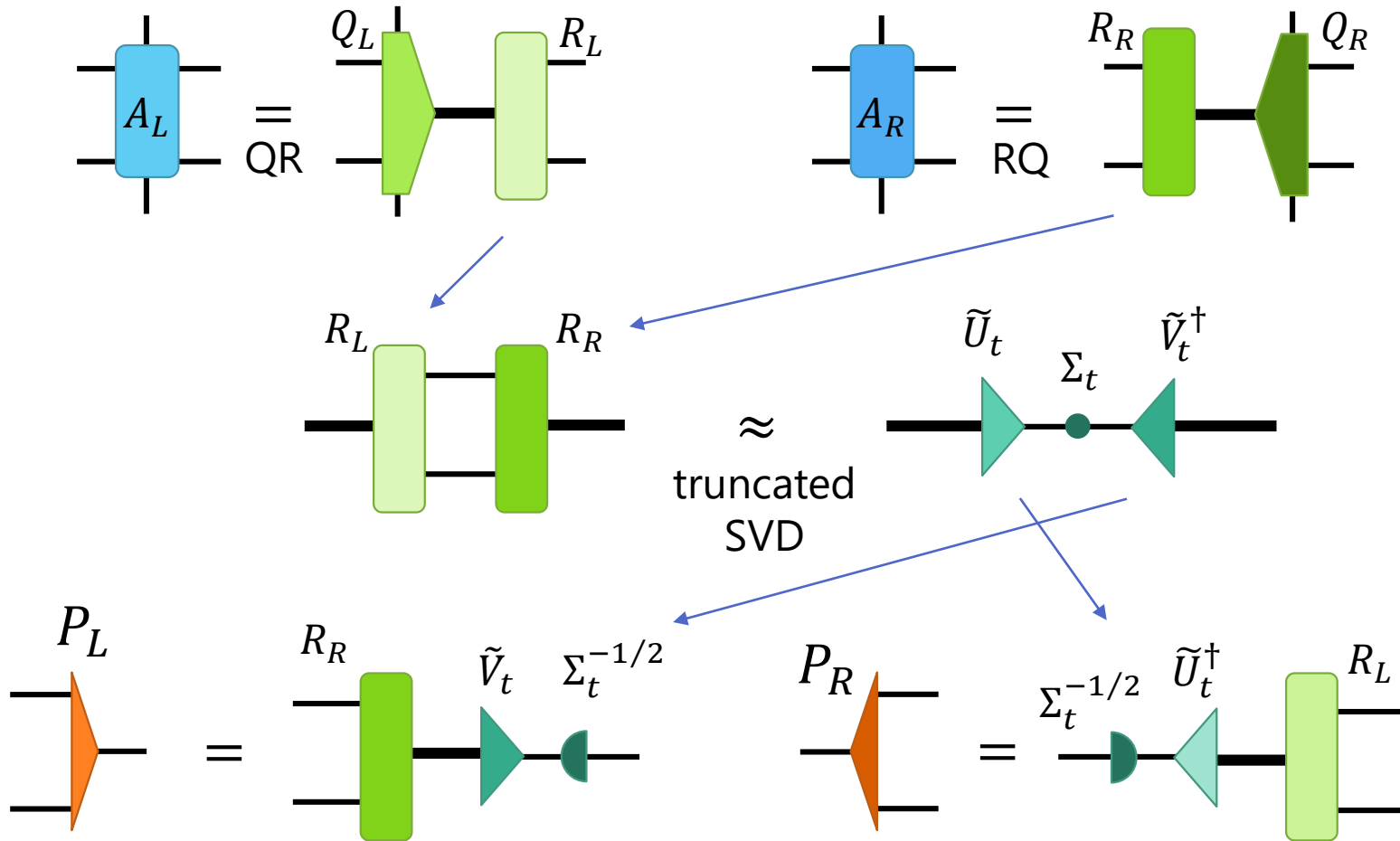
The diagram illustrates the lower bound derivation. It starts with a 2x2 cluster of blue tensors, followed by an equals sign and a light blue rounded square. This is followed by an approximation symbol  $\approx$  and the text "Truncated SVD". To the right is a diagram of a truncated SVD decomposition: a green trapezoid labeled  $U_t$  is connected to a green circle labeled  $\Sigma_t$ , which is then connected to a green trapezoid labeled  $V_t^\dagger$ . To the far right, the inequality  $\Delta \geq \sum_{i>\chi} \sigma_i^2$  is shown.

How do we obtain  $P_L$  and  $P_R$  satisfying the follow conditions?

The diagram shows the decomposition of the projectors. On the left, an orange trapezoid labeled  $P_L$  is shown with an equals sign followed by a green trapezoid labeled  $U_t$  connected to a green semi-circle labeled  $\sqrt{\Sigma_t}$ . On the right, an orange trapezoid labeled  $P_R$  is shown with an equals sign followed by a green semi-circle labeled  $\sqrt{\Sigma_t}$  connected to a green trapezoid labeled  $V_t^\dagger$ .

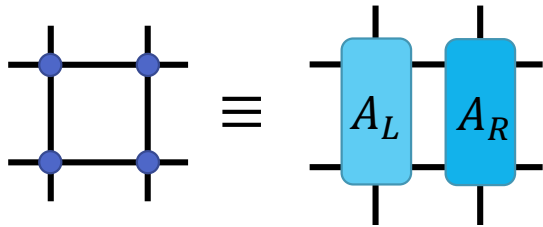
# Algorithm based on QR decomposition

Wang, Verstraete, arXiv:1110.4362, Corboz, Rice, Troyer, PRL **113**, 046402 (2014)



$(P_L P_R)$  is an "oblique" projector

# Derivation of “Oblique” Projector



$$A_L A_R = \underset{\text{SVD}}{U \Sigma V^\dagger} \approx \underset{\text{truncation}}{U_t \Sigma_t V_t^\dagger}$$

$$A_L = Q_L R_L$$

QR decomp.

$$A_R = R_R Q_R$$

RQ decomp.

$$R_L R_R = \underset{\text{SVD}}{\tilde{U} \Sigma \tilde{V}^\dagger} = \underset{\text{truncation}}{\tilde{U}_t \Sigma_t \tilde{V}_t^\dagger}$$

Comparing two SVDs, we obtain

$$U_t = Q_L \tilde{U}_t \quad V_t^\dagger = \tilde{V}_t^\dagger Q_R$$

$$\tilde{U}_t^\dagger = U_t^\dagger Q_L \quad \tilde{V}_t = Q_R V_t$$

$$\begin{aligned} A_L P_L &= U_t \sqrt{\Sigma_t} \quad \times \sqrt{\Sigma} V^\dagger V \Sigma_t^{-1/2} \\ &= U \Sigma V^\dagger V_t \Sigma_t^{-1/2} \\ &= (A_L A_R) V_t \Sigma_t^{-1/2} \\ &= A_L (R_R Q_R) V_t \Sigma_t^{-1/2} \\ &= A_L \underbrace{R_R \tilde{V}_t \Sigma_t^{-1/2}}_{P_L} \end{aligned}$$

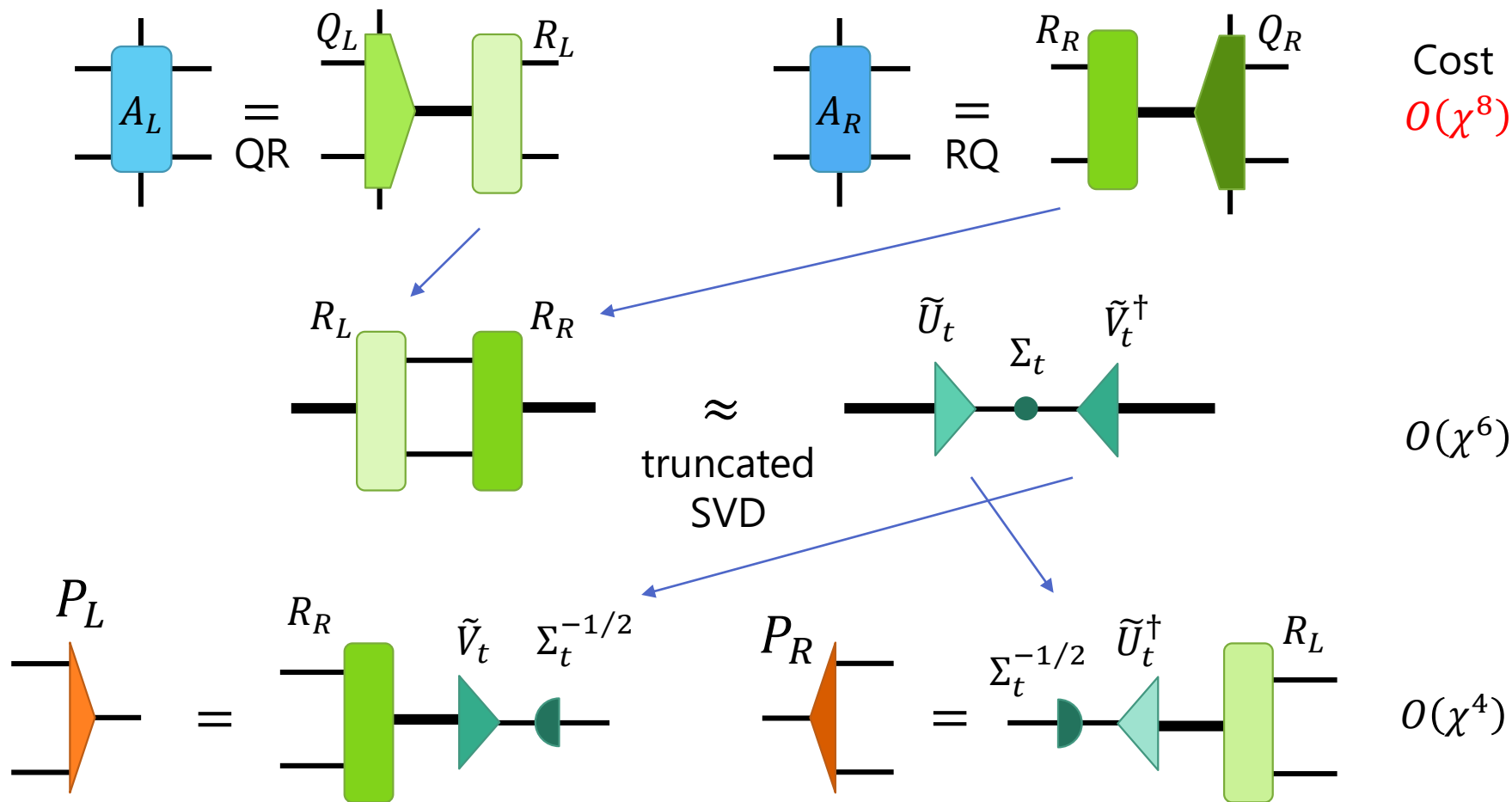
In the same way, we obtain

$$P_R = \Sigma_t^{-1/2} \tilde{U}_t^\dagger R_L$$

We can easily prove  $P_L P_R = (P_L P_R)^2$ .

# Computational Cost

Wang, Verstraete, arXiv:1110.4362, Corboz, Rice, Troyer, PRL **113**, 046402 (2014)



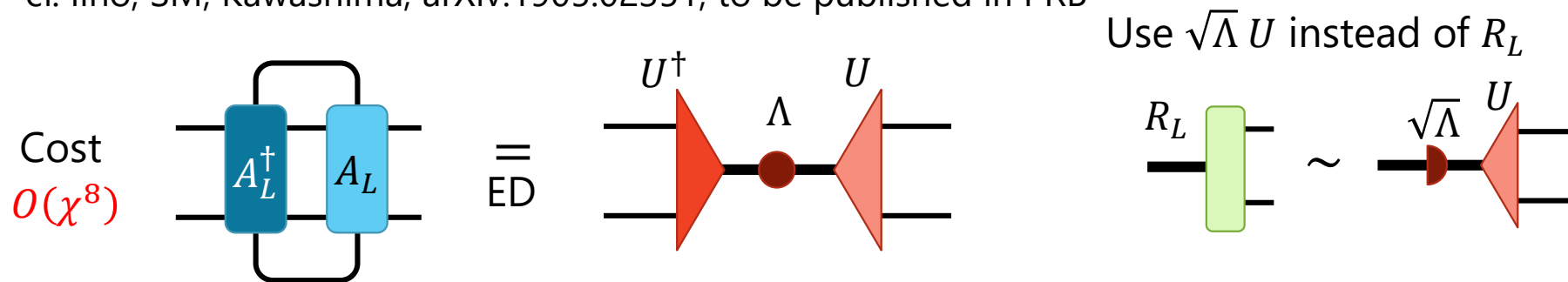
For HOTRG,  $O(\chi^8)$  cost is unacceptable.

We can avoid the QR decomp by using ED because  $Q_L$  and  $Q_R$  is unnecessary.

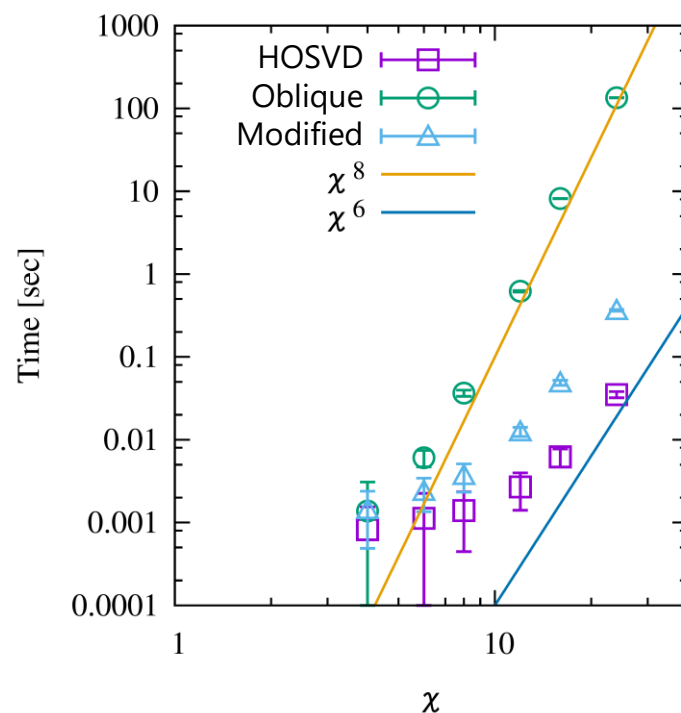
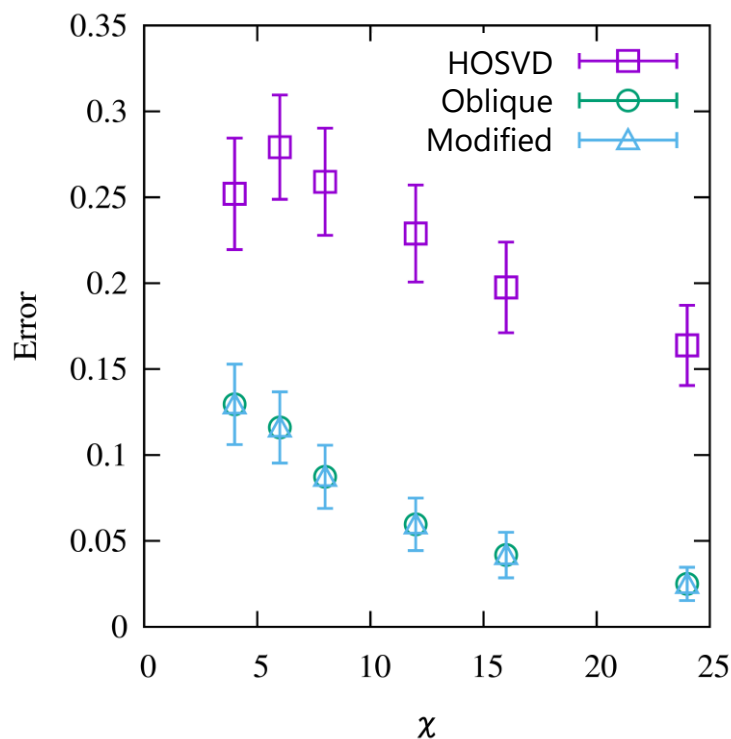


# Modified Algorithm for "Oblique" Projector

cf. lino, SM, Kawashima, arXiv:1905.02351, to be published in PRB



## ➤ Benchmark on random tensors

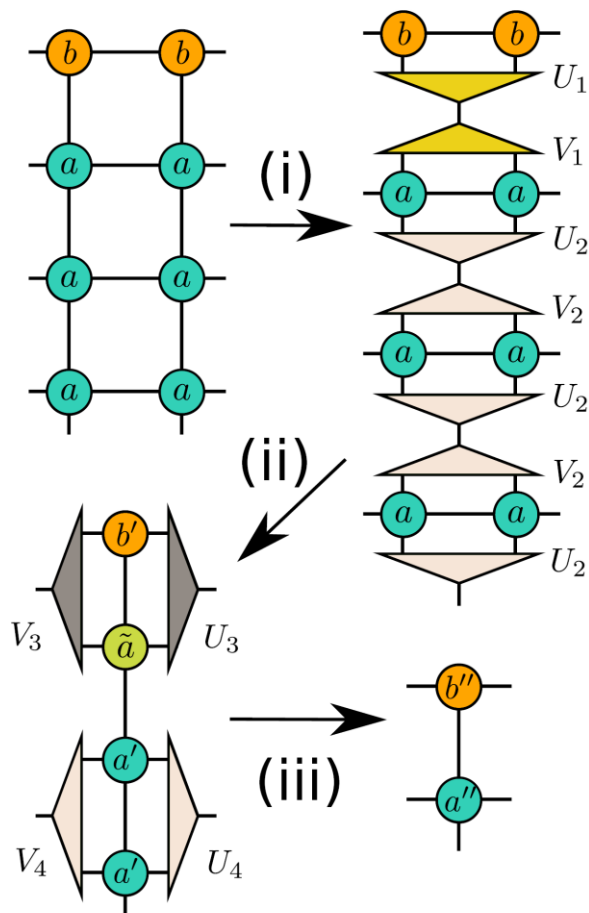


# Boundary Tensor Renormalization Group

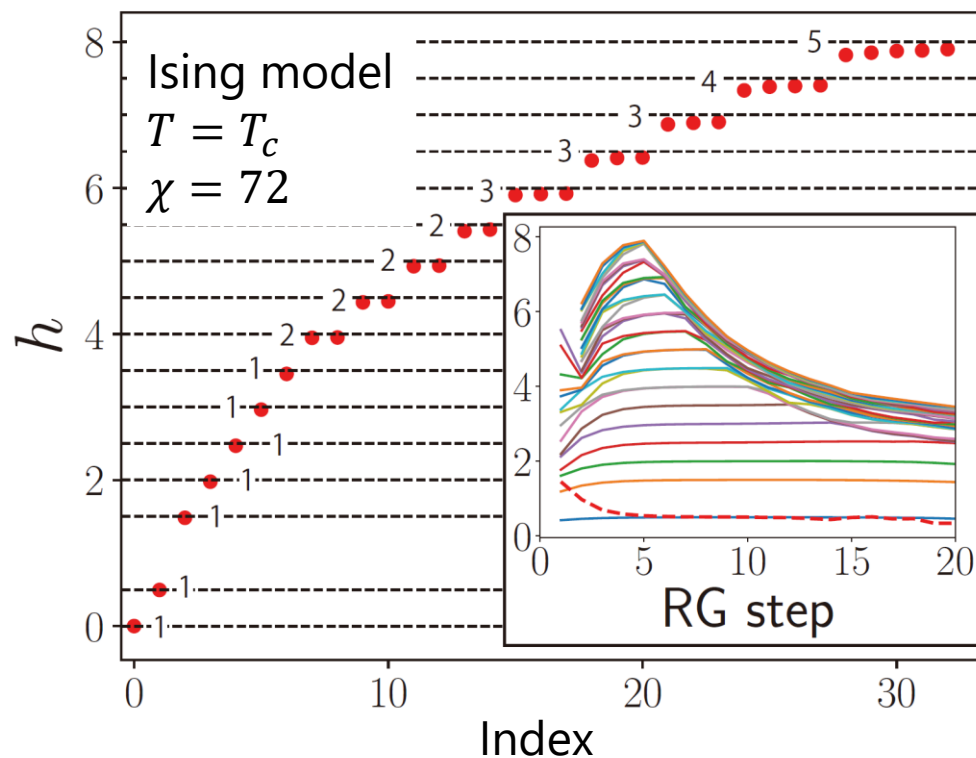
Iino, SM, Kawashima, arXiv:1905.02351, to be published in PRB

Iino's talk  
July 22, 15:30-

## ○ HOTRG with open boundaries



## Scaling dimension of boundary CFT



$$Z_{\text{free,free}} = \chi_0 + \chi_{\frac{1}{2}}$$

**1<sup>st</sup> Part:**

# **Higher-order moments by Higher-order Tensor Renormalization Group**

# Binder ratio

K. Binder: Z. Phys. B **43**, 119 (1981)

$$U_4 \equiv \frac{\langle m^4 \rangle}{\langle m^2 \rangle^2}$$

Magnetization

$$m = \frac{1}{N} \sum_i S_i$$

$$\lim_{T \rightarrow 0} U_4 = 1$$

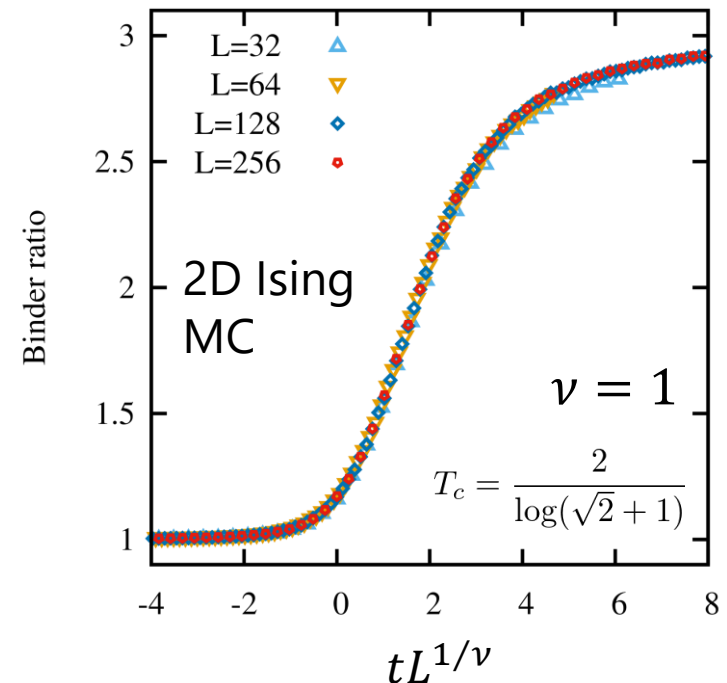
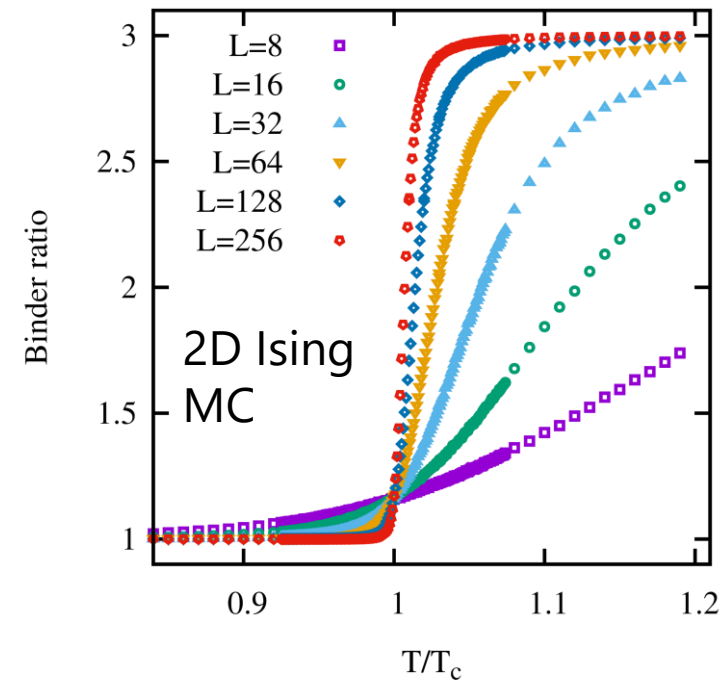
$$\lim_{T \rightarrow \infty} U_4 = 3$$

(Ising model)

- ✓ Dimensionless quantity
- ✓ Step function in  $N \rightarrow \infty$
- ✓ Crossing point  $\rightarrow T_c$

Finite-size scaling analysis

$$U_4(t, L) = \Psi(tL^{1/\nu}) \quad t \equiv \frac{T - T_c}{T_c}$$



# Order parameter $\langle m \rangle$

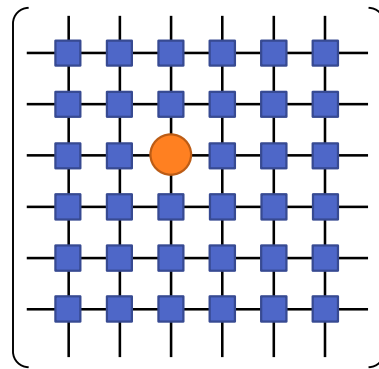
## 1. Derivative of free energy

$$\langle m \rangle = -\frac{\partial f}{\partial h}$$

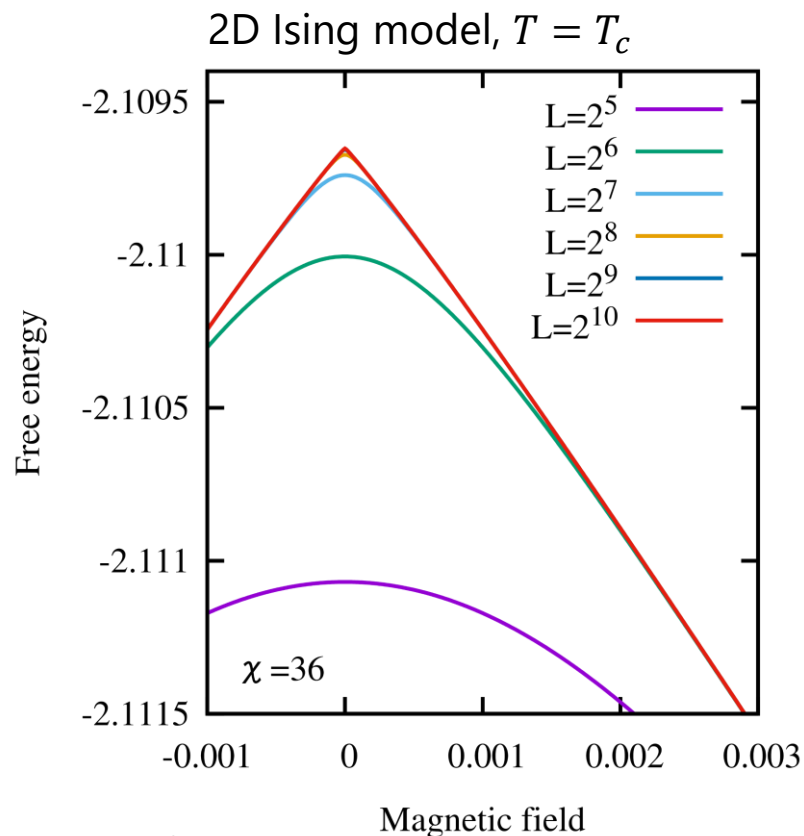
- Error from numerical differential approximation.
- External field breaks symmetry of tensor.

## 2. Impurity tensor

$$\text{Tr } S_i e^{-\beta H} = \text{tTr}$$

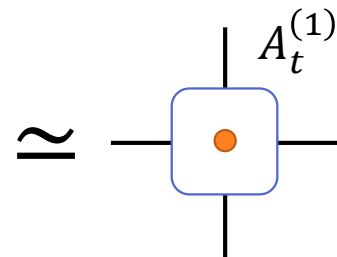
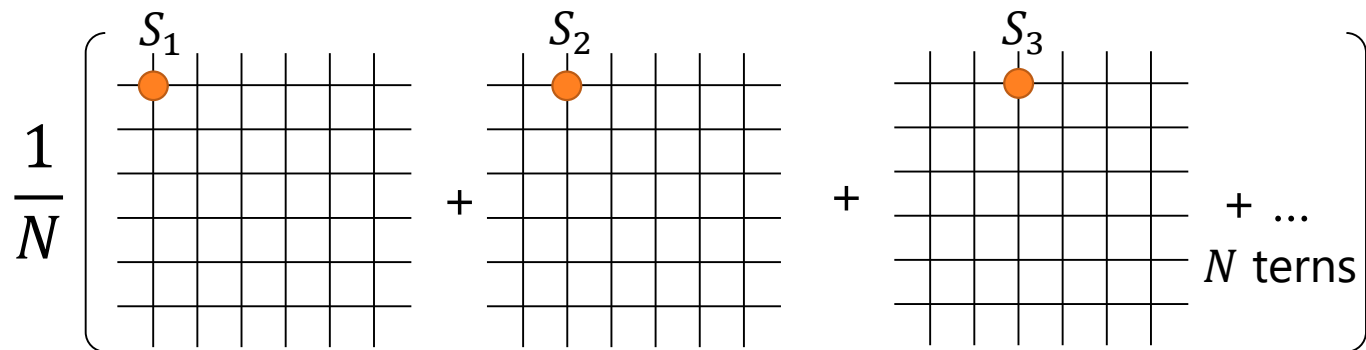


Multi-point correlations are necessary for high-order moments  $\langle m^n \rangle$ .

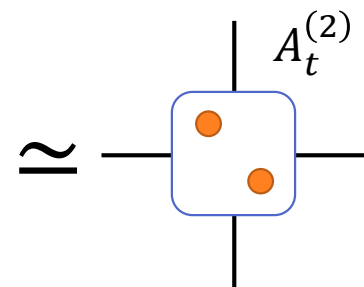
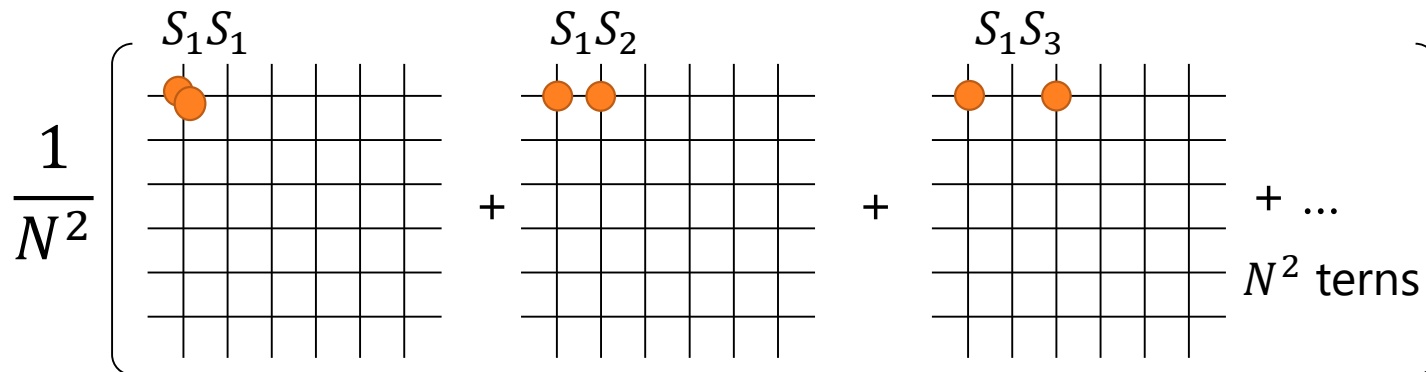


# Multipoint correlation functions

- 1<sup>st</sup>-order moment  $\left\langle \frac{1}{N} \sum_{i=1}^N S_i \right\rangle$  "the average of the local operators"

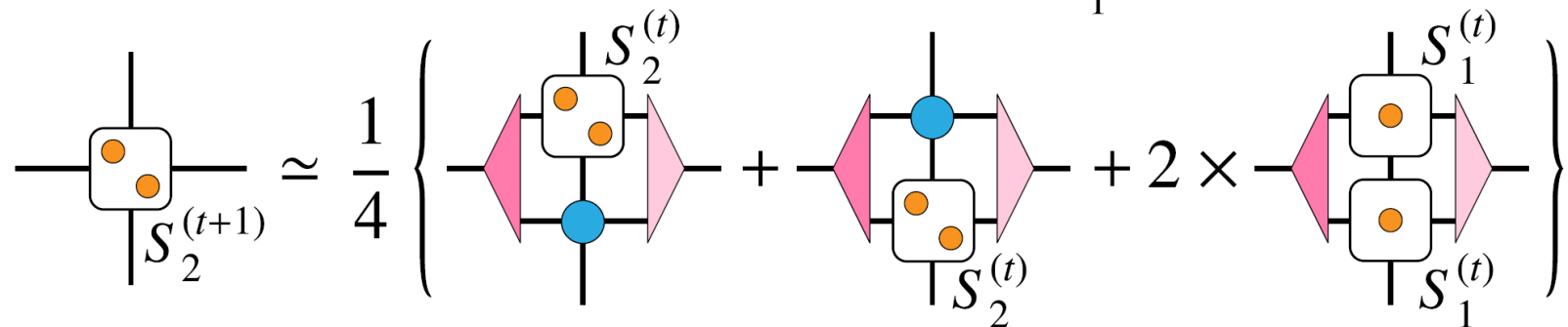
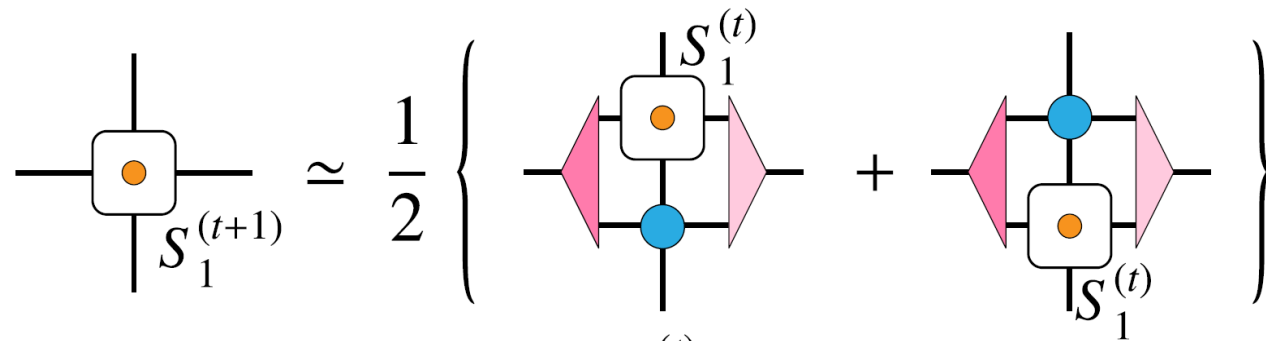
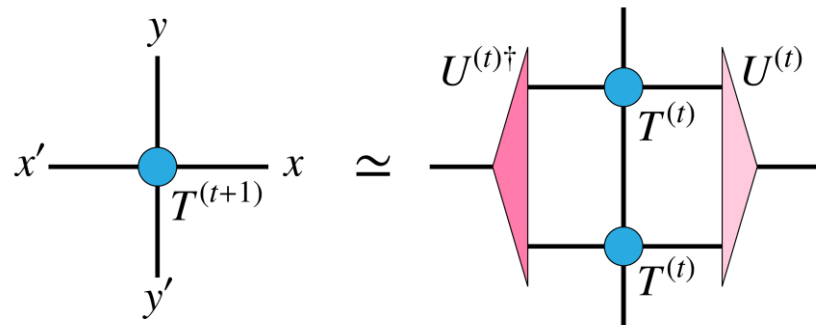


- 2<sup>nd</sup>-order moment  $\left\langle \frac{1}{N^2} \sum_{i,j} S_i S_j \right\rangle$



We calculate the renormalized tensor of the summation of multipoint correlation functions by using HOTRG.

# Renormalization of multi-impurity tensors



# Renormalization of multi-impurity tensors

$$\begin{array}{c} \text{---} \square \text{---} \\ | \\ S_1^{(t+1)} \end{array} \simeq \frac{1}{2} \left\{ \begin{array}{c} S_1^{(t)} \\ | \\ \text{---} \square \text{---} \\ | \\ \text{---} \square \text{---} \\ | \\ S_1^{(t)} \end{array} + \begin{array}{c} \text{---} \square \text{---} \\ | \\ S_1^{(t)} \\ | \\ \text{---} \square \text{---} \\ | \\ \text{---} \square \text{---} \\ | \\ S_1^{(t)} \end{array} \right\}$$

$$\begin{array}{c} \text{---} \square \text{---} \\ | \\ S_2^{(t+1)} \end{array} \simeq \frac{1}{4} \left\{ \begin{array}{c} S_2^{(t)} \\ | \\ \text{---} \square \text{---} \\ | \\ \text{---} \square \text{---} \\ | \\ S_2^{(t)} \end{array} + \begin{array}{c} \text{---} \square \text{---} \\ | \\ S_2^{(t)} \\ | \\ \text{---} \square \text{---} \\ | \\ \text{---} \square \text{---} \\ | \\ S_2^{(t)} \end{array} + 2 \times \begin{array}{c} S_1^{(t)} \\ | \\ \text{---} \square \text{---} \\ | \\ \text{---} \square \text{---} \\ | \\ S_1^{(t)} \end{array} \right\}$$

$$S_3 \leftarrow \frac{1}{8} (S_3 T + 3S_2 S_1 + 3S_1 S_2 + T S_3)$$

$$S_4 \leftarrow \frac{1}{16} (S_4 T + 4S_3 S_1 + 6S_2 S_2 + 4S_1 S_3 + T S_4)$$

- Use the same isometry  $U^{(t)}$  for the local tensor  $T^{(t)}$
- Generalization for multiple kinds of impurities



# 2D $q$ -state classical Potts model

$$H = -J \sum_{\langle ij \rangle} \delta_{\sigma_i, \sigma_j} - h \sum_i \delta_{\sigma_i, 0}$$

$$(\sigma_i = 0, 1, \dots, q-1)$$

We consider  $h = 0$ .

○ Phase transition at  $T_c = \frac{J}{\log(\sqrt{q} + 1)}$

➤  $q \leq 4$  : 2<sup>nd</sup>-order

➤  $q > 4$  : 1<sup>st</sup>-order

➤ Correlation length

$q$	4	5	6	7	8	9	10
$\xi$	$\infty$	2512.2	158.9	48.1	23.9	14.9	10.6

Weakly 1<sup>st</sup>-order

# TN representation

## ○ Local tensor

$$T_{xyx'y'}^{(0)} = \frac{\sqrt{\lambda_x \lambda_y \lambda_{x'} \lambda_{y'}}}{q} \delta_{x+y, x'+y'}^{[q]}$$

$Z_q$  symmetry

$$x + y - x' - y' \equiv 0 \pmod{q}$$

$$\lambda_x = e^K - 1 + q\delta_{x,0}$$

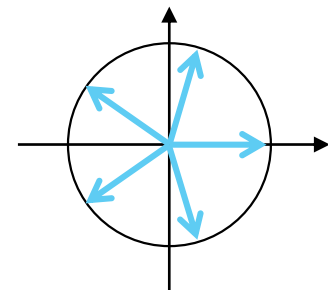
Eigen value of local Boltzmann factor  $W_{\sigma,\sigma'} = e^{K\delta_{\sigma,\sigma'}}$

## ○ Order parameter

### ➤ Complex magnetization

$$m = \frac{1}{N} \sum_{i=1}^N \exp \left[ i \frac{2\pi}{q} S_i \right]$$

$$U_4 \equiv \frac{\langle |m|^4 \rangle}{\langle |m|^2 \rangle^2}$$



### ➤ Impurity tensor for $m^k m^{*k'}$

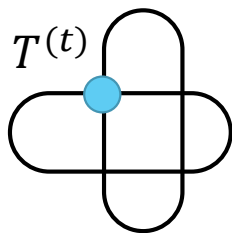
$$S_{k,k';xyx'y'}^{(0)} = \frac{\sqrt{\lambda_x \lambda_y \lambda_{x'} \lambda_{y'}}}{q} \delta_{x+y+k, x'+y'+k'}^{[q]}$$

Covariant with spin rotation (charge  $k - k'$ )

$$x + y - x' - y' \equiv k - k' \pmod{q}$$

# Magnetization

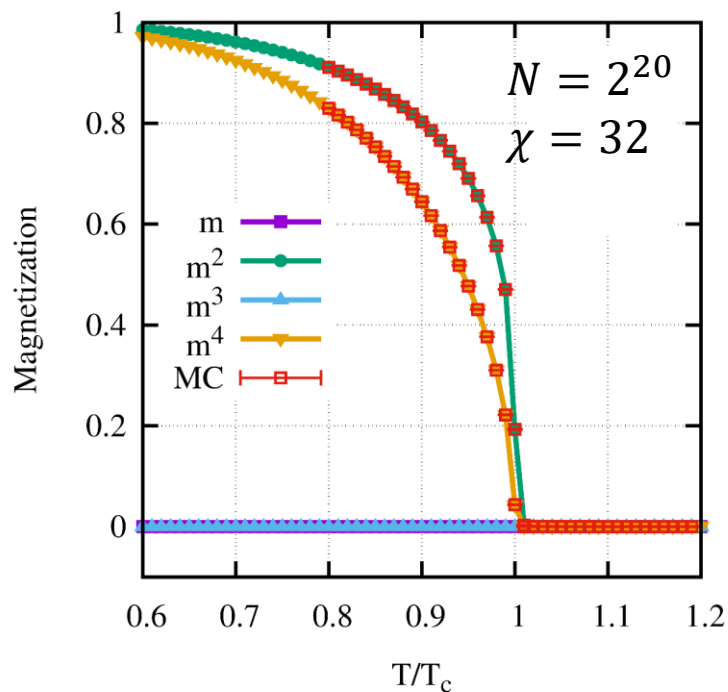
$$\langle |m|^2 \rangle_N \simeq \frac{\text{Tr } S_{1,1}^{(t)}}{\text{Tr } T^{(t)}}$$



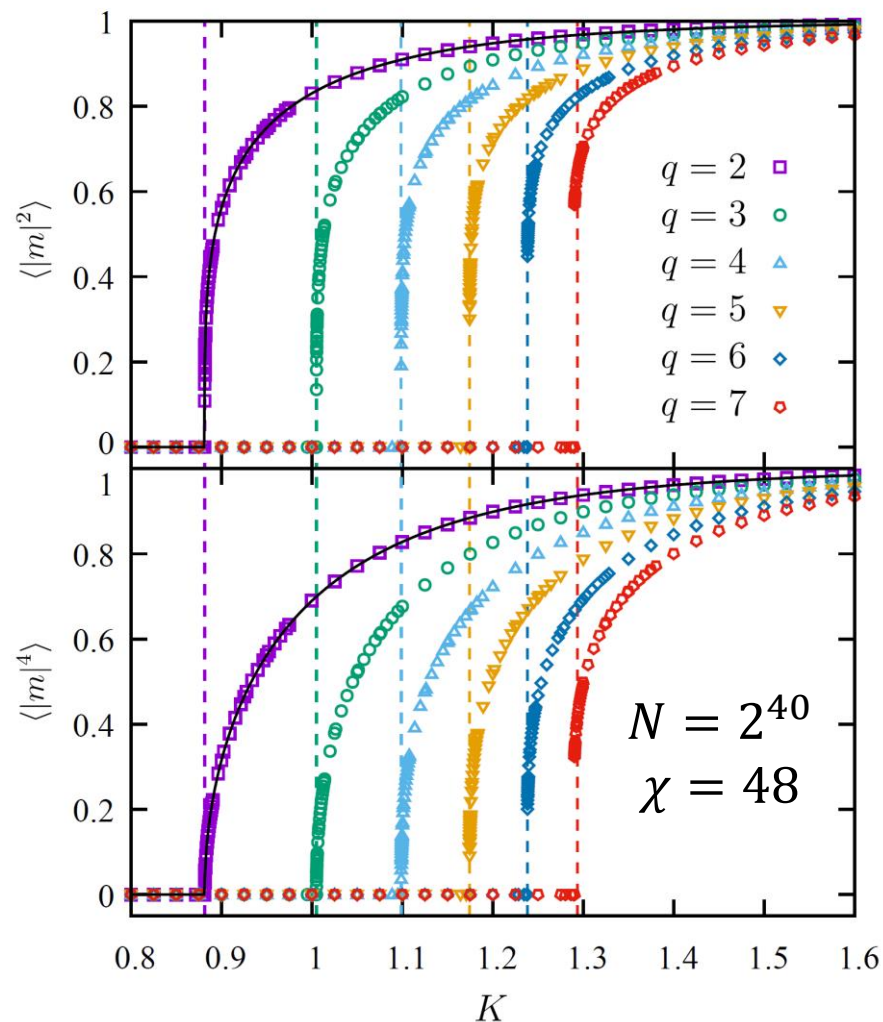
$$\text{Tr } T^{(t)} = \sum_{x,y} T_{xyxy}^{(t)}$$

Periodic BC  
 $N = 2^t$

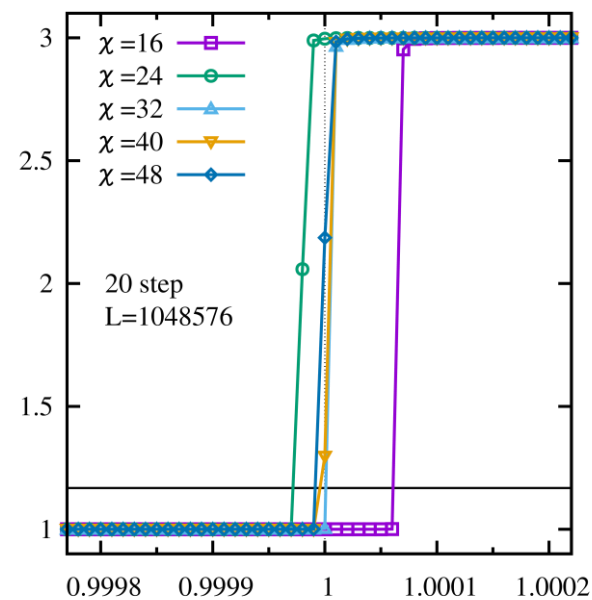
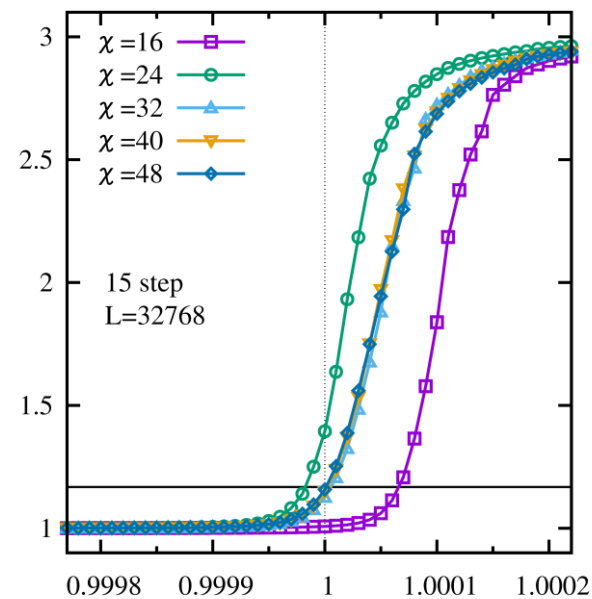
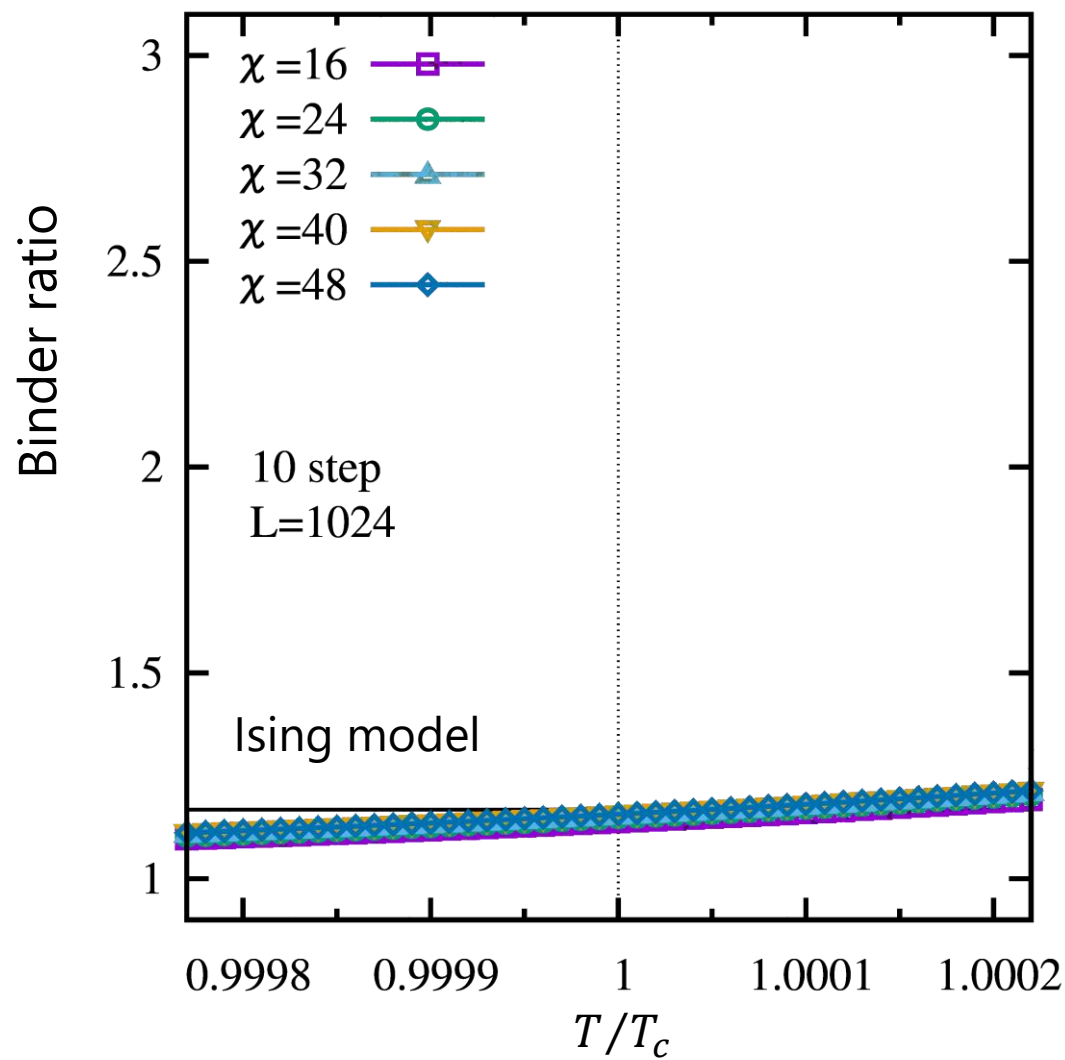
## ➤ Ising model ( $q = 2$ )



## ➤ $q$ -state Potts model

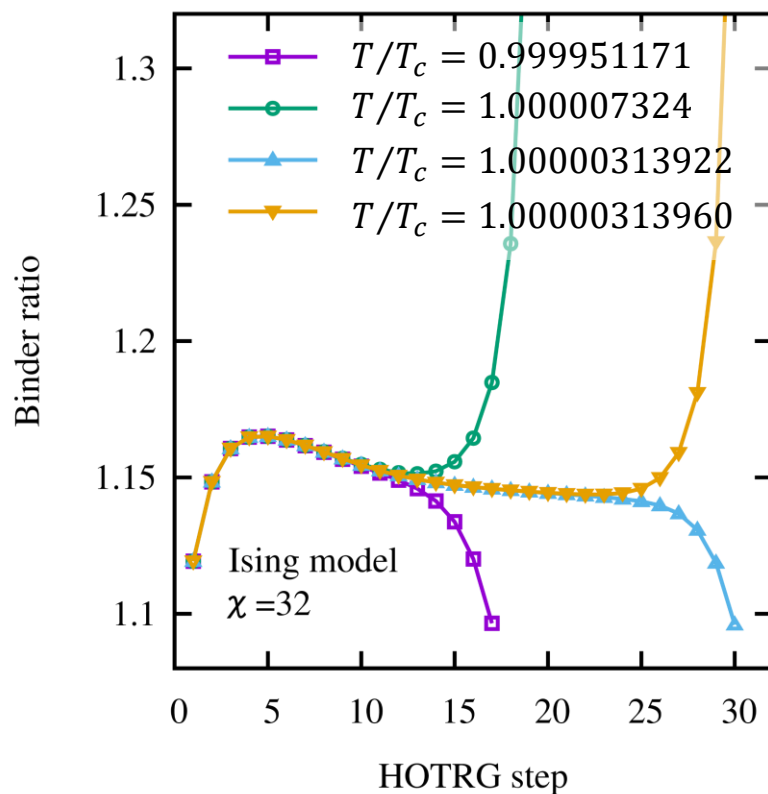


# $\chi$ -dependence

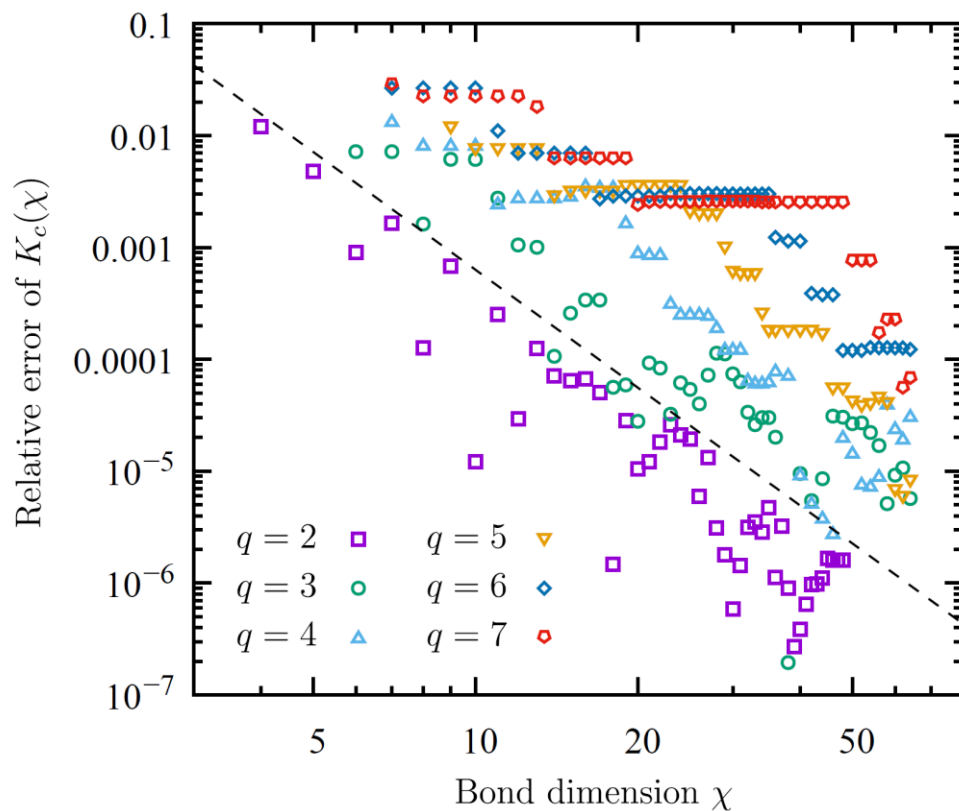


# Transition temperature

## Bisection search



## $\chi$ -dependence



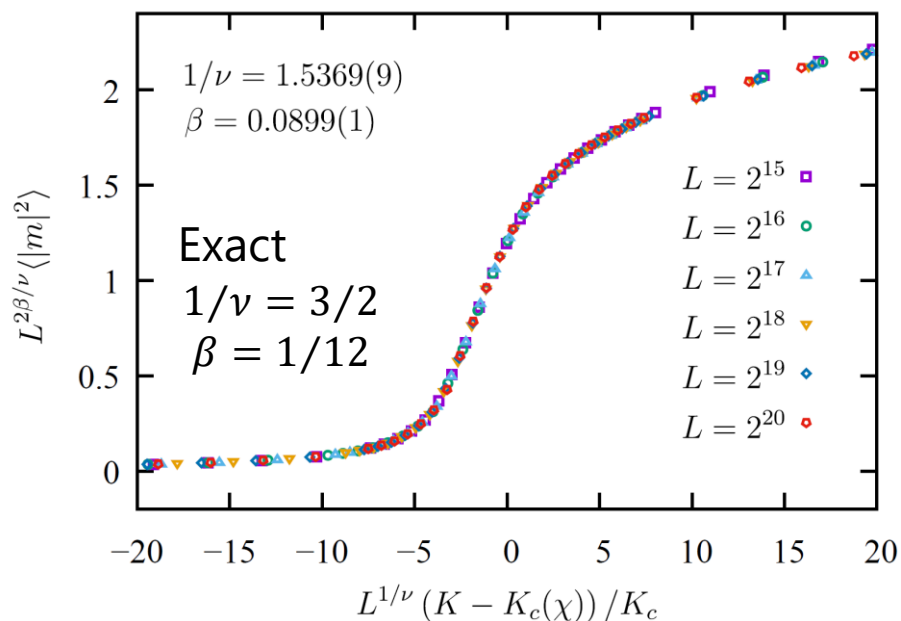
- Estimated values converge to the exact value with oscillation
- Relative error seems to decay in proportion to  $\chi^{-3.5}$

# Finite-size scaling analysis

$$\langle |m|^2 \rangle \sim L^{-2\beta/\nu} g(L^{1/\nu} \delta)$$

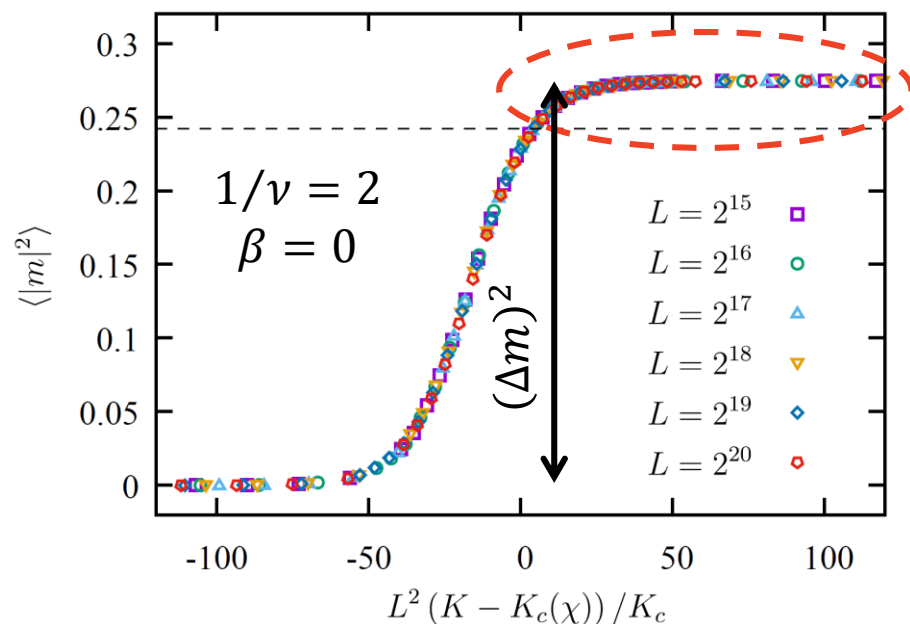
$$\delta \equiv (K - K_c(\chi))/K_c$$

4-state Potts model



- ✓ Fitting by Bayesian scaling (Harada, 2011)
- ✓ Effect of logarithmic correction is small

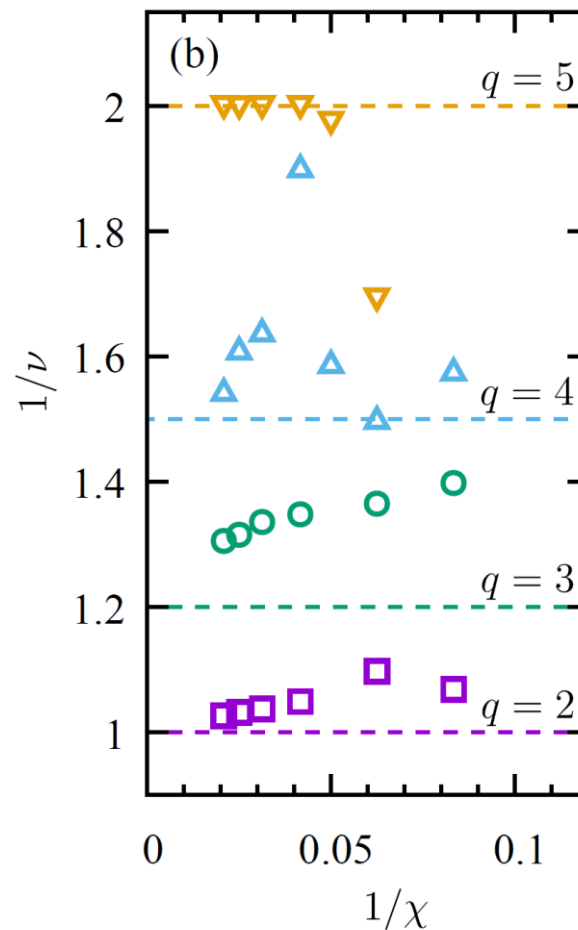
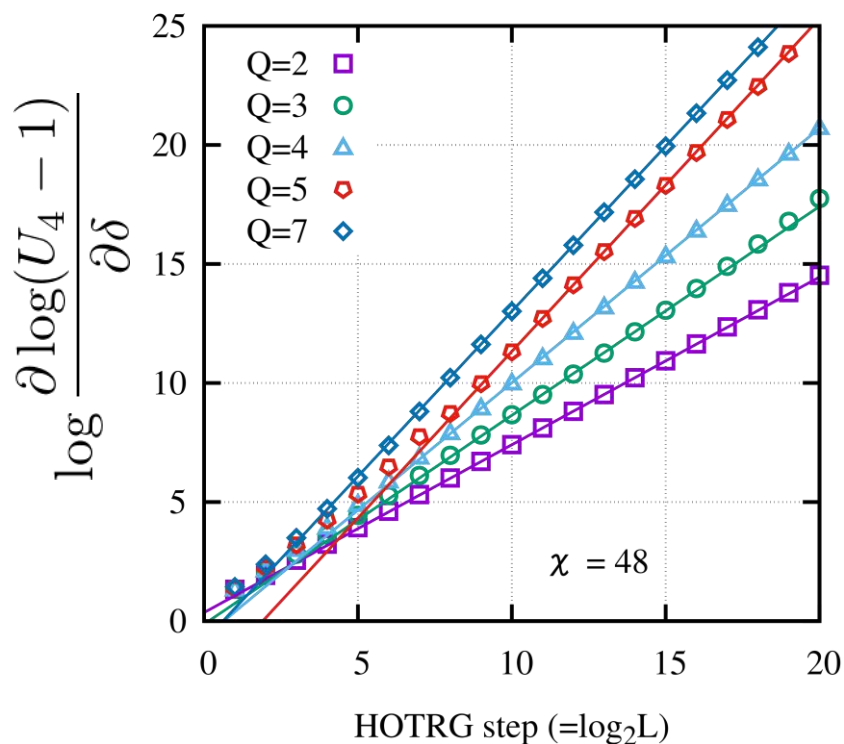
5-state Potts model



- ✓ No fitting
- ✓ Plateau indicate the 1<sup>st</sup>-order phase transition.

# Slope of Binder ratio

$$\log \left| \frac{\partial U_4}{\partial \delta} \right|_{\delta=0} = a + \frac{1}{\nu} \log L + \dots$$



$q$	2	3	4	5	7
Exact	1	6/5	3/2	2	2
Slope	1.026(2)	1.305(10)	1.544(1)	2.006(2)	2.0001(5)

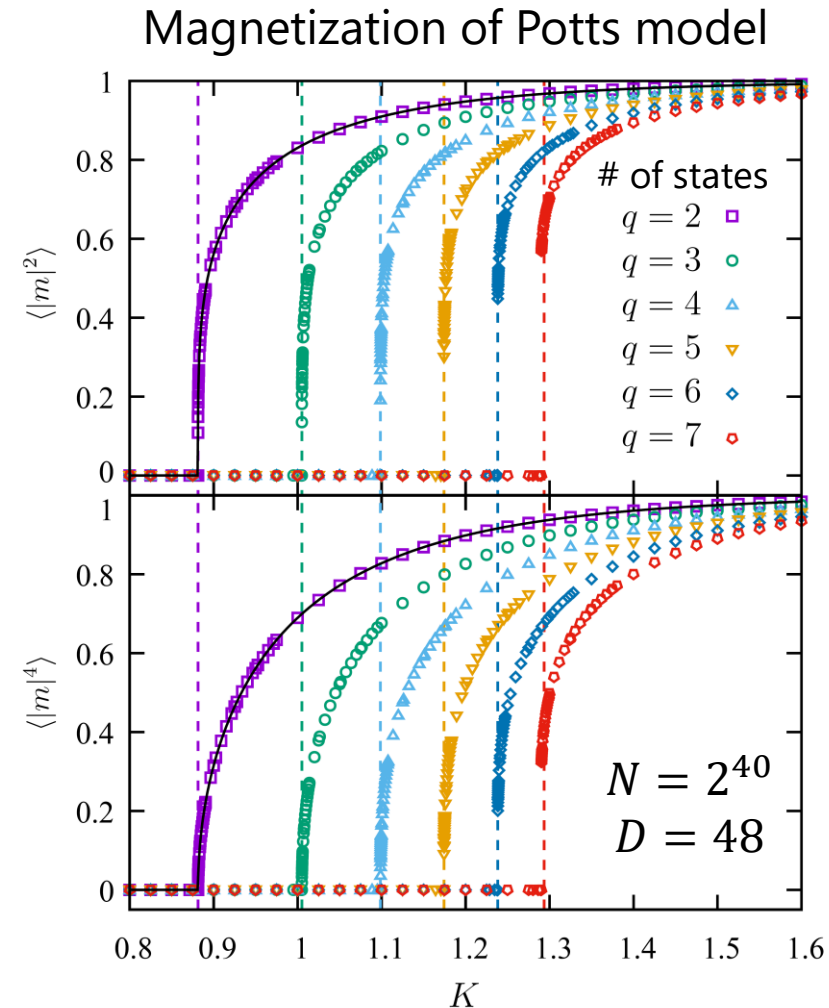
# Summary of the 1<sup>st</sup> part

## ○ Renormalization of tensors with multiple impurities

$$\begin{aligned} \text{Tensor } S_1^{(t+1)} &\approx \frac{1}{2} \left\{ \text{Diagram 1} + \text{Diagram 2} \right\} \\ \text{Tensor } S_2^{(t+1)} &\approx \frac{1}{4} \left\{ \text{Diagram 3} + \text{Diagram 4} + 2 \times \text{Diagram 5} \right\} \end{aligned}$$

The diagrams represent tensor contractions. Diagram 1 shows a square tensor with one orange dot (top) and one blue dot (bottom), with two pink triangles on its horizontal legs. Diagram 2 shows a square tensor with one blue dot (top) and one orange dot (bottom), with two pink triangles on its horizontal legs. Diagram 3 shows a square tensor with two orange dots (top) and one blue dot (bottom), with two pink triangles on its horizontal legs. Diagram 4 shows a square tensor with one blue dot (top) and two orange dots (bottom), with two pink triangles on its horizontal legs. Diagram 5 shows two square tensors stacked vertically, each with one orange dot, and two pink triangles on the horizontal legs of the top tensor.

- ✓ Beyond the system size which the Monte-Carlo method can treat.
- ✓ Finite-size scaling analysis of the magnetization and the Binder ratio.
- ✓ Distinguish weakly first-order and continuous phase transitions



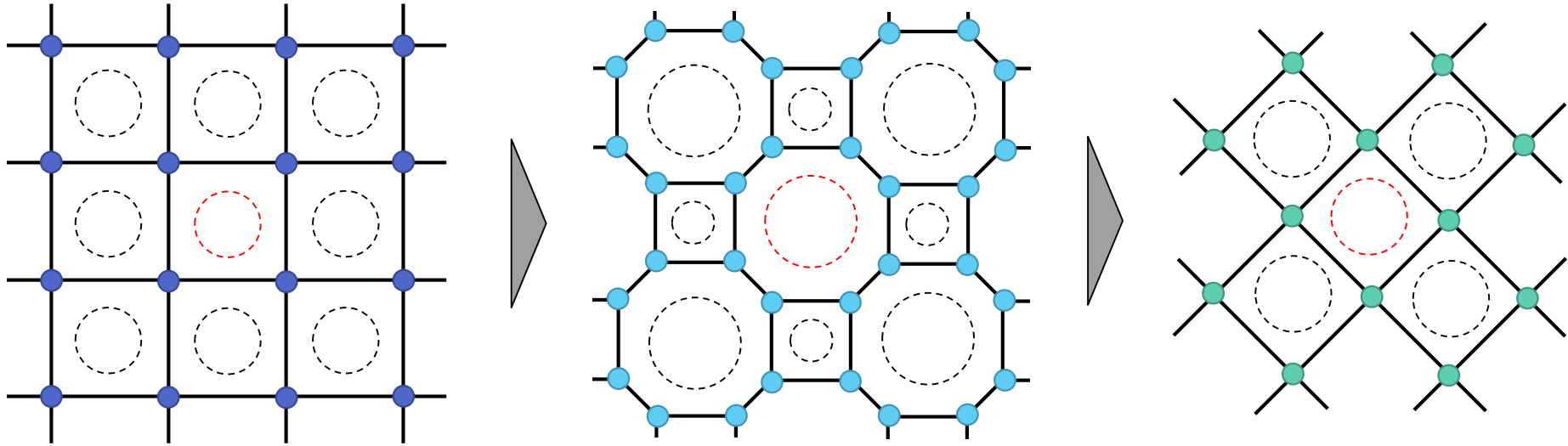


## **2<sup>nd</sup> Part:**

# **HOTRG with entanglement filtering**

Unpublished results are removed in this part.

# Internal Correlations

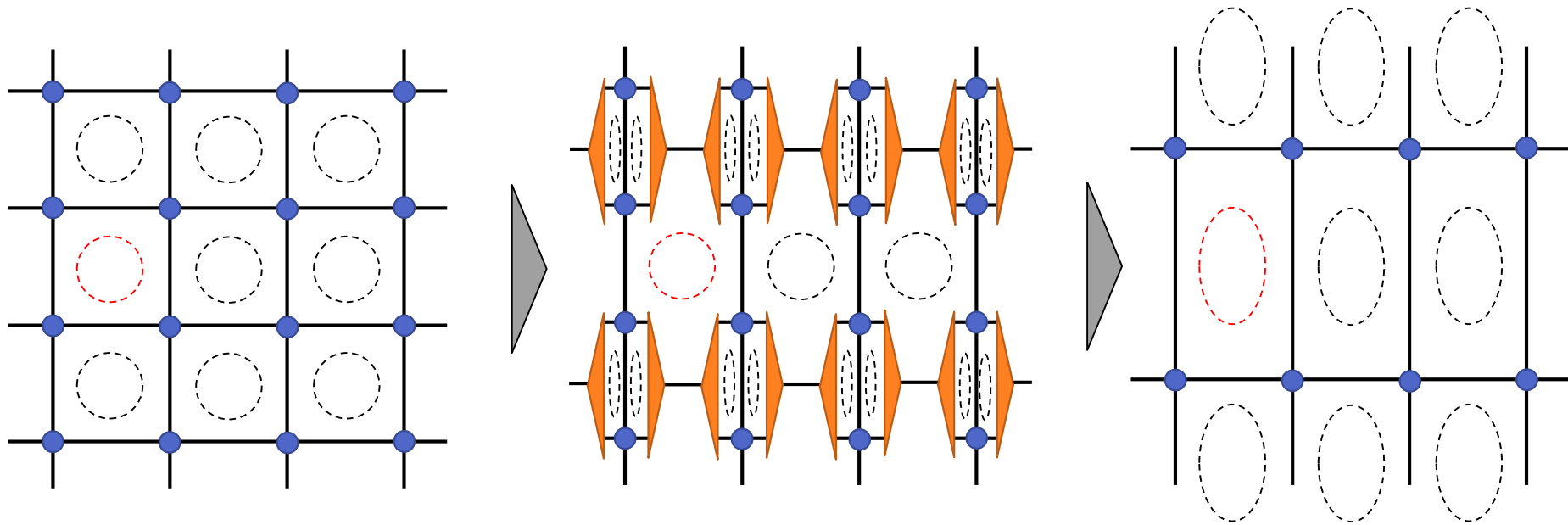


- Irrelevant correlations with  $O(1)$  length scale
- Converge to a fictitious fixed-point tensor
  - Corner Double Line structure

We need to remove internal correlations within a loop.

**“Entanglement Filtering”**

# Internal Correlations



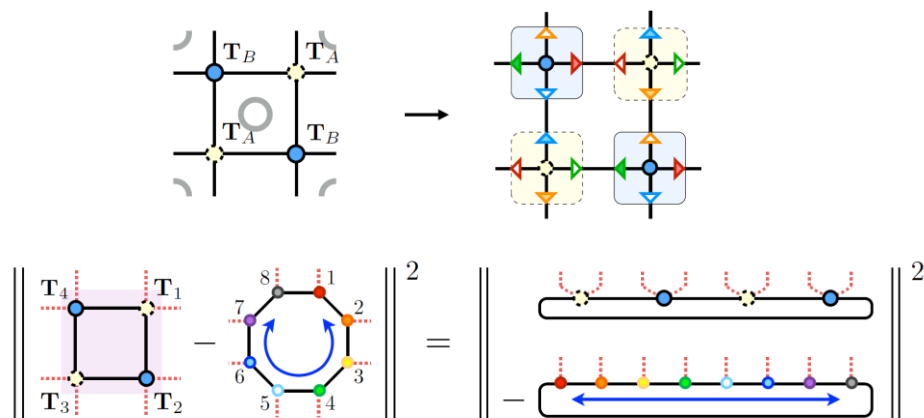
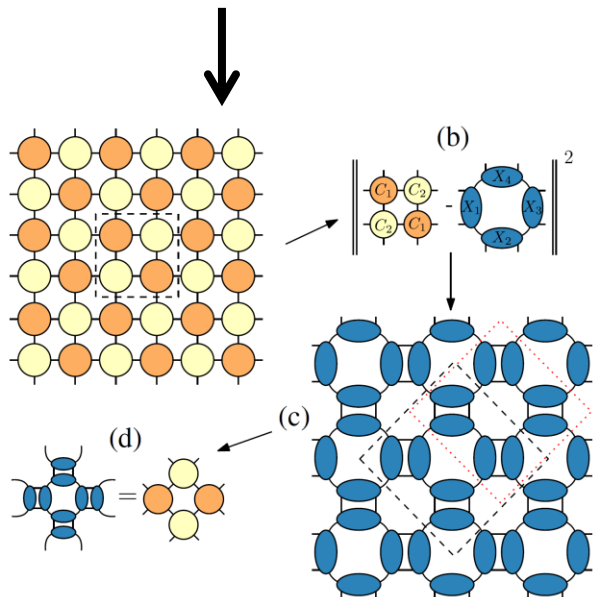
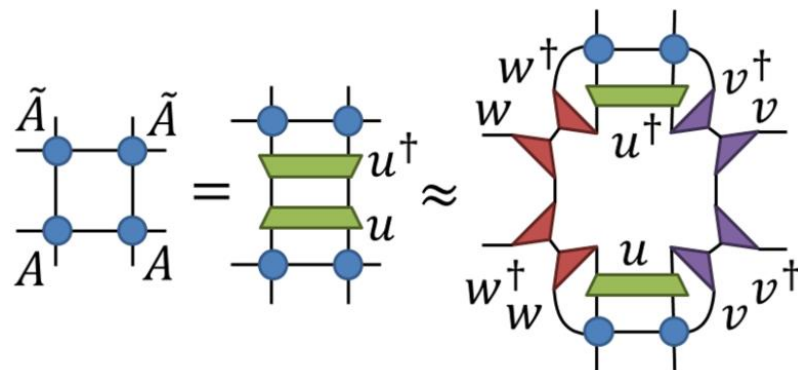
- Irrelevant correlations with  $O(1)$  length scale
- Converge to a fictitious fixed-point tensor
  - Corner Double Line structure Gu, Wen (2009)

We need to remove internal correlations within a loop.  
**“Entanglement Filtering”**

# TRG with Entanglement Filtering

## ○ TRG-base methods

- **TEFT** [Gu, Wen (2009)]
- **TNR** [Evenbly, Vidal (2015)]
- **loop-TNR** [Yang, Gu, Wen (2017)]
- **TNR+** [Bal, et al, (2017)]

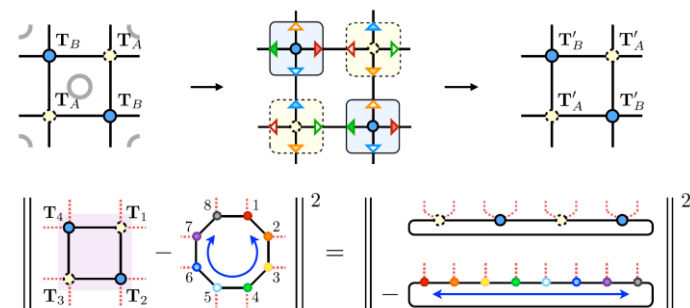
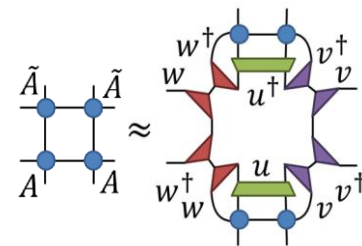


Only for 2-d systems

# Entanglement Filtering

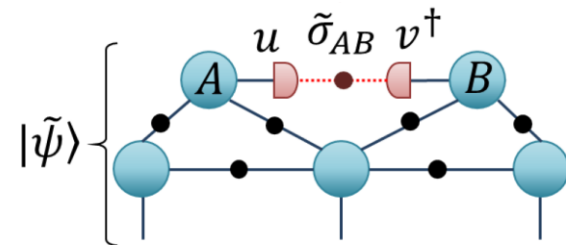
## ○ TRG-base methods Only for 2-d systems

- TEFT [Gu, Wen (2009)]
- TNR [Evenbly, Vidal (2015)]
- loop-TNR [Yang, Gu, Wen (2017)]
- TNR+ [Bal, et al, (2017)]



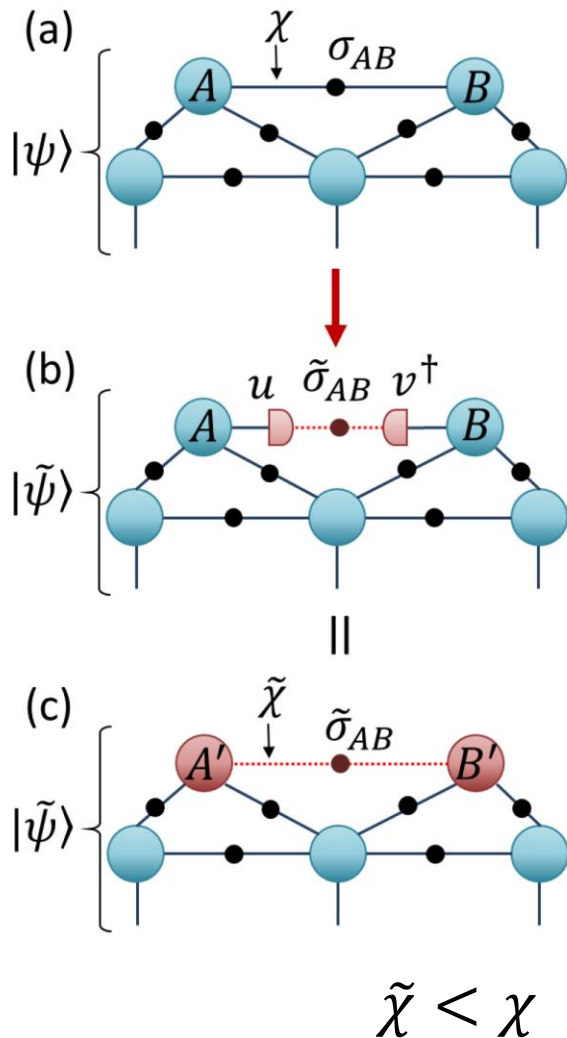
## ○ General methods

- Graph Independent Local Truncation [Hauru, Delcamp, Mizera (2017)]
- Tensor Network Skeletonization [Ying (2016)]
- Entanglement Branching [Harada (2018)]
- Full Environment Truncation [Evenbly (2018)]



We consider a combination with HOTRG and FET.

# Full Environment Truncation (FET)

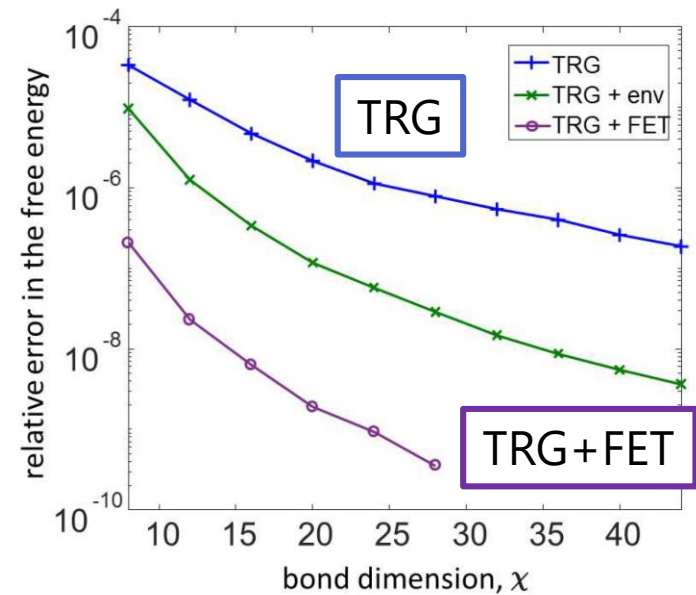


✓ Simple criterion

Optimize isometries  $u, v$  and bond diagonal matrix  $\tilde{\sigma}_{AB}$  to minimize the difference

$$\left\| |\psi\rangle - |\tilde{\psi}\rangle \right\|^2$$

✓ TRG + FET



**Thank you for your attention!**